Middle East Journal of Applied Sciences
Volume: 16 | Issue: 03| July – Sept. | 2026

EISSN: 2706 -7947 ISSN: 2077- 4613
DOI: 10.36632/mejas/2026.16.3.12
Journal homepage: www.curresweb.com
Pages: 161-185

Mineralogy and Radioactivity of Gabal El-Urf-Abu Shiht Area Stream Sediments, North Eastern Desert, Egypt

S. M. El Alfi

Nuclear Materials Authority, P.O. Box: 530 El Maadi, Cairo, Egypt.

Received: 20 April 2026 **Accepted:** 30 June 2026 **Published:** 15 July 2026

ABSTRACT

The area covered by basement rocks represented by metavolcanics, older granite, younger gabbro, and younger granite, pegmatites and dikes. The area covered by 25 samples of stream sediments, Wadi Abu Shih covered by 15 samples and wadi Abu Shihat covered by 10 samples. The total heavy minerals ranging from 4.056% to 6.521% with an average of about 5.148% in wadi Abu Shih and ranging from 3.243% to 4.752% with an average of about 4.187% in wadi Abu Shihat. The total heavy economic minerals ranging from 1.716% to 4.634% with an average of about 2.898% in wadi Abu Shih and ranging from 1.254% to 1.813% with an average of about 1.5825% in wadi Abu Shihat. The radioactive minerals represented by samarskite, thorite, columbite and fluorite. The eU examined in the stream sediments of Wadi Abu Shih ranges from 4 ppm to 25 ppm, with an average 13.93 ppm, while eTh ranging from 12 ppm to 60 ppm, with an average 30.13 ppm, Ra ranging from 4 ppm to 19 ppm, with an average 8.53 ppm and K% ranging from 1.4% to 2.6 %, with an average 2.12%. The eU examined in the stream sediments of Wadi Abu Shihat ranges from 5 ppm to 9 ppm, with an average 6.5 ppm, while eTh ranging from 11 ppm to 16 ppm, with an average 13.7 ppm, Ra ranging from 5 ppm to 9 ppm, with an average 6.9 ppm and K% ranging from 1.1% to 3.3 %, with an average 1.91%. The variation diagrams between radioactive elements shows the low alteration processes affecting on the samples in wadi Abu Shih while shows the high alteration processes affecting on the samples in wadi Abu Shihat.

Keywords: Mineralogy, radioactivity, Gabal El-Urf, stream sediment, granites, pegmatite

1. Introduction

G. El-Urf and G. Abu Shihat area (about 90km^2) is located in the north of Qena-safaga asphaltic road at km 85 from Qena in the North Eastern Desert of Egypt between latitudes 26° 35` and 26° 40` N, and longitudes 33° 20` and 33° 30` E. The area is covered by basement rocks and is characterized by high rugged mountains. The highest elevations in the study area are G. El Urf (989m. a.s.l). The area is crossed by two wadis the first is Abu Shih from the south and the second is Abu Shihat from the North, these wadis trending NE-SW. They are relatively wide, sinuous and filled by placer deposits as sand and gravels from the country rocks which formed the shoulders of these wadis. The two wadis drained their load into Wadi Ghubb As-Salam, which the later drained their load into wadi Fatirah and the later drained their load into wadi Qena and finally into the River Nile (Fig. 1).

The area was extensively studied by many workers since it was discovered by El-Taher (1978). Several geological and radiometric studies were carried out in order to explore the uranium mineralizations as Bishady *et al.,* (1999); Abdel Ghani (2001); El-Mansi and Dardier (2005), Khamis (2012); Asran *et al.,* (2013), Anas 2015 and El Dabe *et al.,* (2022 a,b). Habib (1982) who investigated the mineralized granites in the area including G. El Missikat, G. El Urf and Ria El Garra, using digital processing and Landsat MSS data using ratio of bands and color enhancement techniques. He believed such signatures reflect hydrothermal halos of possible mineralized quartz veins.

Corresponding Author: S. M. El Alfi, Nuclear Materials Authority, P.O. Box: 530 El Maadi, Cairo, Egypt.
E-mail: samehelalfi2@gmail.com

Habib (1987) studied the geologic and metallogenic significance of pan African photo-lineaments in the central Eastern Desert. He concluded that the NNE-SSW to NE-SW and NW-SE trends are particularly significant. They have guided the intrusion of large volumes of granitic magmas and hydrothermal mineralization such as Au, U, Cu and W.

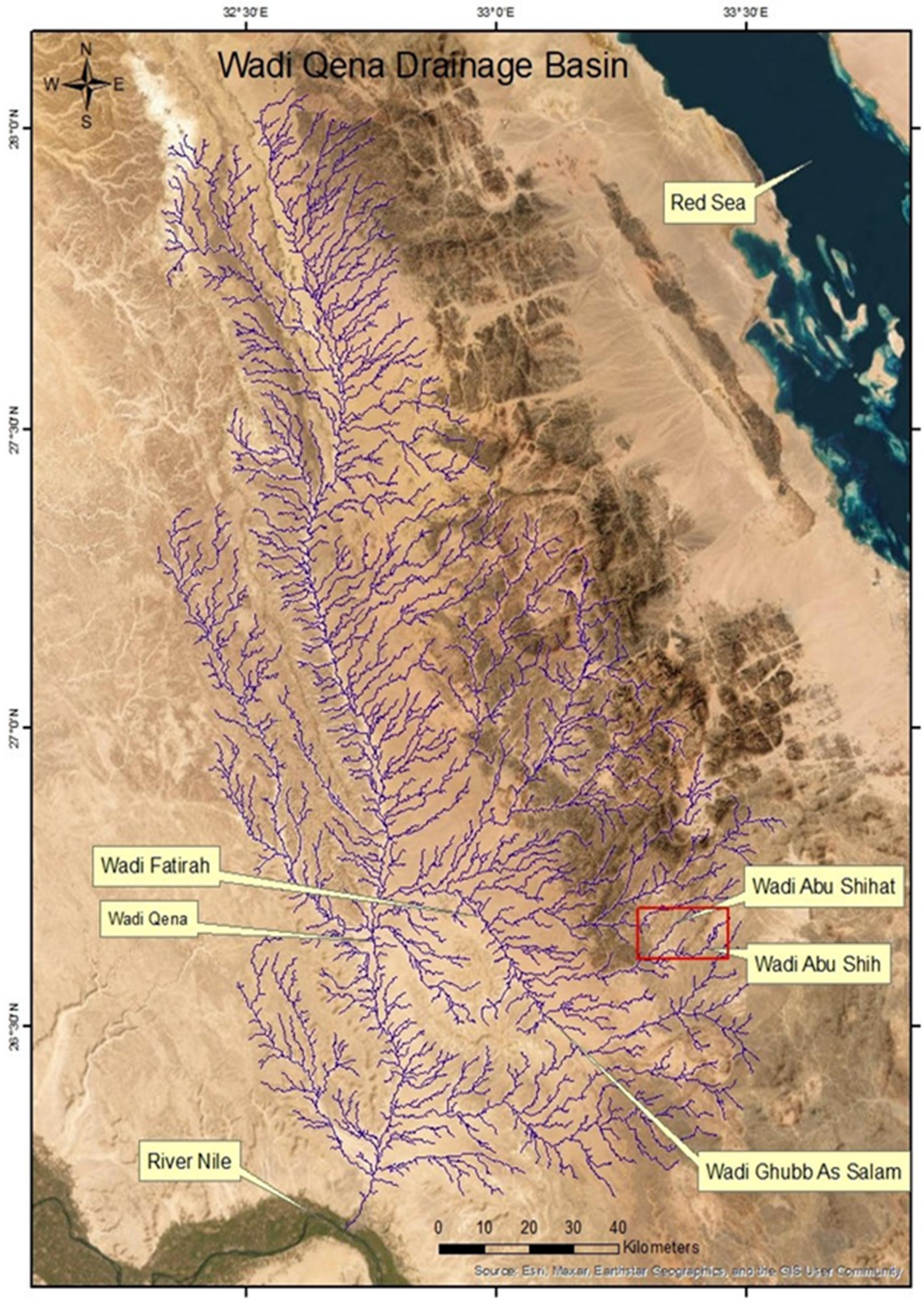


Fig. 1: The drainage pattern of wadi Qena basin

Geologic Setting

The study area covered by different basement rocks represented by Metavolcanics, Older Granitoids, younger gabbro, and younger granite, pegmatites and dikes. These rocks arranged from old to young as follows;

Metavolcanics

This rock located in western part of study area and intruded by younger granites which split him into two parts one to north and the second to south (Fig. 2). Metavolcanic show fault contact with older granites from NE and E. (Fig. 3a).

Older Granitoids

Crop out in the vast area around G. El Urf and G. Abu Shihat (Fig. 2). The older granitoids are usually form low-lying separate hills (Fig. 3b). They represented by quartz diorite and granodiorite. Their colors range from whitish to dark grey, generally medium to coarse-grained and composed mainly of plagioclase and quartz, together with variable proportions of potash feldspars, biotite and hornblende. Sericite, epidote, chlorite and muscovite are common secondary accessories (El-Gaby and Habib 1982; Abdel Ghani 2001; EL-Mansi and Dardier 2005). Older granites show fault contact with metavolcanics from SW, and intrude in it from the NW. They are intruded by younger granites; their contacts are sharp intrusive contact. They may contain abundant X-Foliation and xenoliths of older basic rocks (Fig. 3c&d).

Younger Gabbro

They are exposed as a large part in the study area. They crop out in the north part (Fig. 2). These rocks occur as huge batholith intruding the older rocks granite and intruded by younger granites of G. El-Urf with intrusive sharp contact. They are medium to coarse grained, range in color from grayish green to dark gray, massive in some parts and intensively weathered in others (Fig. 3e). The weathered surfaces vary in color from deep brown to violet brown. The rocks are intensively jointed.

Younger Granites

This rock Crop out in the study area form the masses of G. El Urf- Abu Shihat, and form an elongated belt of high relief trending NE (Fig. 2), with circular to ovoid outlines. They are commonly massive and grayish pink to red color. They form sharp intrusive contacts against the surrounding older granitoids.

EL-Mansi and Dardier (2005) stated that: younger granites petrographically classified in to syenogranites (grayish pink varieties of Gabal El-Urf) (Fig. 3f) and Alkali feldspar granites (red varieties of Gabal Abu Shihat) (Fig. 3g). The contact between them is usually inferred, but several small offshoots of red granites invade the greyish pink varieties. Generally, alteration of the younger granites is mainly represented by hematization, which renders the granites brick-red color. Other minor alteration features as epidotization, chloritization, silicification and kaolinization are restricted to fault and joint planes.

Pegmatites

El Mansi and Dardier 2005 are subdivided the pegmatite into:

1- Zoned pegmatites are dominate in G. El-Urf as small sub rounded pockets and mainly composed of quartz surrounded by K-feldspars, while mica is absent or very rare.
2- The unzoned pegmatites are dominate along the southwestern corner of G. Abu Shihat as large size elongated pockets (Fig. 3h), and composed of intergrowth of quartz and K-feldspars with large flakes of muscovite. The fractures of quartz are usually filled with iron oxy-hydroxides and dissemination of metallic black and waxy yellow minerals.

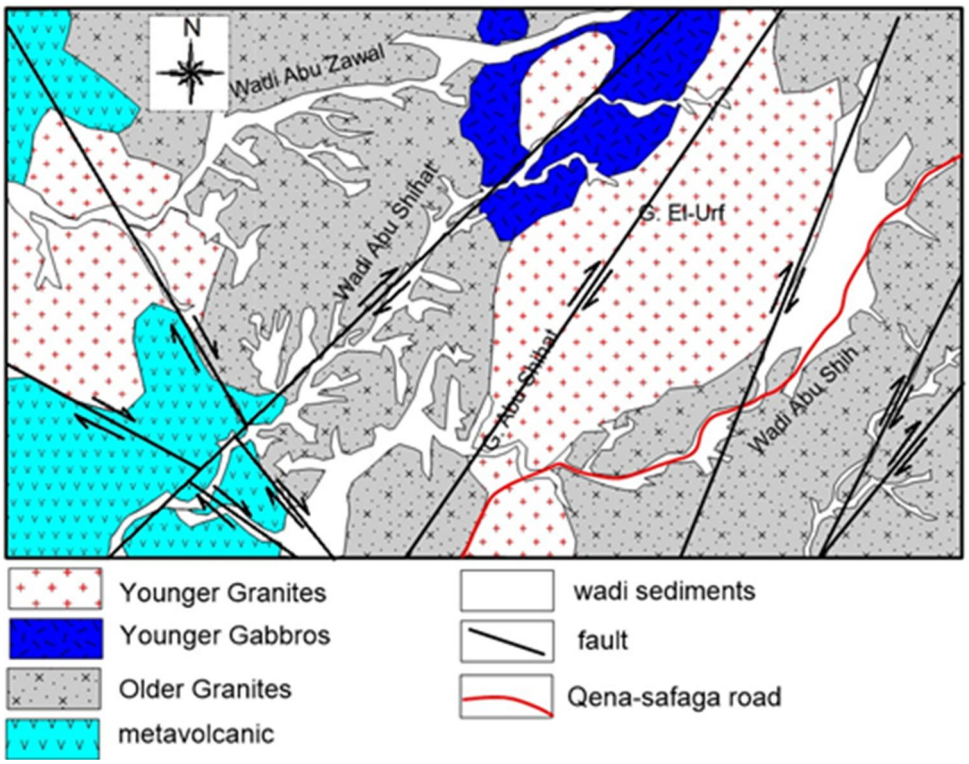


Fig. 2: Geologic map of Gabal El-Urf – Gabal Abu Shihat area, Eastern Desert, Egypt (after Anas, 2015).

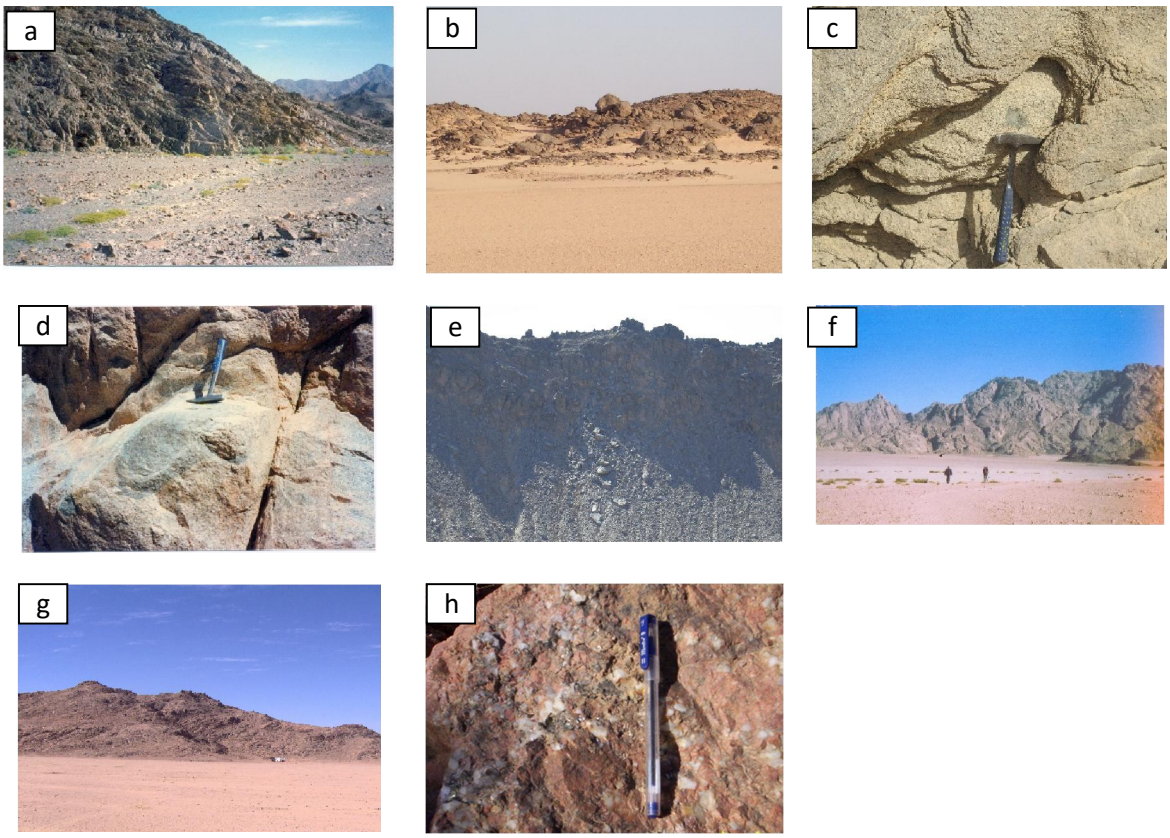


Fig. 3: Photomicrograph shows: a) Metavolcanic, b) Low Hills of Older Granite, c) Xenolith of Older Rock and X-Foliation in Older Granite, d) Older Granitoid with xenolith of metavolcanic, e) Younger Gabbro, f) El Urf Younger Granite, g) G. Abu Shihat Younger Granit and h) Unzoned Pegmatite in G. Abu Shihat younger Granite

Asran *et al*., (2013) and Anas (2015) are concluded that, the pegmatites are classified mineralogically and genetically as simple and complex. Simple pegmatites have simple mineralogy and no zoning, whereas complex pegmatites have their minerals arranged in a zonal sequence and many contain assemblages of rare minerals. Most pegmatites are small, varying from a few feet to tens of feet in longest dimension.

2. Materials and Methods

The present work deal mainly with the mineralogy of the stream sediments. The area covered by 25 samples of stream sediments from the area. Wadi Abu Shih covered by 15 samples and wadi Abu Shihat covered by 10 samples (Fig. 4). They are obtained from pore holes which are 50 cm in diameter, and 1m depth (Fig. 5a &b), at intervals ranging from 900m to 1000m. The average weight of each sample is about 5 kg.

Sampling, Preparation of Samples and Techniques

All mineral species with a specific gravity of more than 2.86g/cm^3 are traditionally considered as heavy minerals. Mohamed (1998) stated that the total heavy minerals were concentrated in the medium, fine and very fine sand size fractions. The air-dried original sample is sieved using a 2mm screen. The separated fraction is quartered using June's splitters of different chutes, the sample was down to about 250 gm. The purified samples are sieved through 0.80mm and 0.063mm screens to remove the coarse sand and silt size fractions. The average weight of the sample prepared for mineral separation is about 60gm. The original sand sample was dried, and prepared for mineral separation using bromoform (Sp. Gr. 2.86 g/cm^3). Heavy fractions were dried, weighted and their percentages were calculated and tabulated in Table (1). The light fractions were discarded, while the heavy fraction is used for further analysis.

The magnetite separation carried out using a small hand magnet with suitable strength. The magnetite free heavy minerals assemblage was magnetically fractionated using the laboratory Frantz Isodynamic Magnetic Separator (Model L-1) at side slope of 5°, forward slope of 20° (Flinter,1955). Mineralogical investigation of the mineral constituents was carried out by Semi-quantitative EDX and the chemical analyses were carried out using a Phillips XL-30 Environmental Scanning Electron Microscope (ESEM) on individual grains of heavy minerals.

3. Results and Discussion

The separated heavy minerals were then studied under a Binocular Stereomicroscope and were classified into two main groups according to Folk (1980). The first is the opaque as; magnetite, ilmenite, leucoxene and hematite the second is the non-opaque include zircon, garnet, monazite, rutile, titanite, gahnite and green silicates (pyroxene and amphibole groups, epidote and mica group) and accessory minerals as pyrite, atacamite, cassiterite and apatite. The percentage of each mineral is calculated to the original samples and averages of the total economic heavy mineral for the studied sediments are tabulated in Table (2).

Opaque minerals

Magnetite (Fe^{2+}, Fe_2^{3+} O_4)

Magnetite habit ranges from massive, granular, angular, sub-angular to sub-rounded (Fig.6a) and the octahedron crystals with parallel twining of magnetite are less frequent and occur as isolated grains (Fig. 6b). some of magnetite grains shows different degrees of alteration (Fig. 6c). Picked pure magnetite grains were investigated under the Environmental Scanning Electronic Microscope (ESEM) and the elemental chemical compositions are shown in figure (6d&e).

Magnetite was recorded in all studied sediments and its content range from 0.43% to 0.87% with an average of 0.653% in wadi Abu Shih and range from 0.21% to 0.48% with an average of 0.333% in wadi Abu Shihat (Table 2).The lateral distribution of magnetite percentages illustrated in (Fig. 7), and show the high concentration at the west and the middle parts beside G. Abu Shihat While the low concentration located at the eastern part in wadi Abu Shih while the concentration decrease gradually from the east to the west in wadi Abu Shihat.

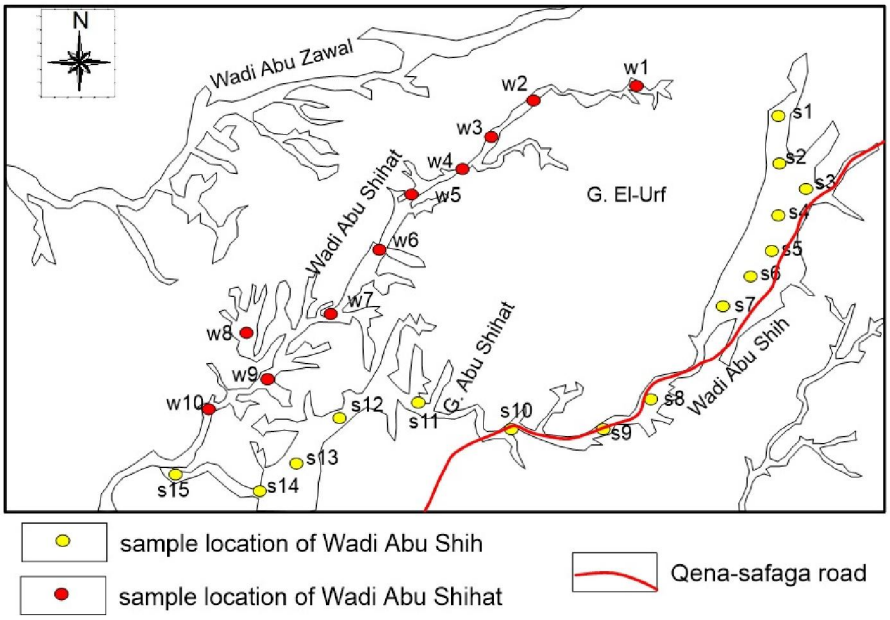


Fig. 4: Shows the distribution of samples in Wadi Abu Shih and wadi Abu Shihat.



Fig. (5a&b): Open bit

Table 1: The Percentages of the Total Heavy Minerals in the studied stream sediments of the area.

S. No.	H. Br. %	S. No.	H. Br. %
S1	4.987	**W1**	3.645
S2	5.231	**W2**	3.859
S3	4.513	**W3**	4.436
S4	5.452	**W4**	4.631
S5	5.563	**W5**	4.647
S6	5.462	**W6**	4.344
S7	4.495	**W7**	4.752
S8	5.637	**W8**	4.238
S9	5.734	**W9**	3.243
S10	6.342	**W10**	4.077
S11	6.521		
S12	4.776		
S13	4.222		
S14	4.056		
S15	4.223		
Min.	4.056		3.243
Max.	6.521		4.752
Aveg.	5.148		4.187

H.Br. = Heavy Bromoform

Table 2: The weight percentages of the concentrated economic heavy minerals in the studied stream sediment samples

S. No.	Mag.	Ilm.	Hem.	Gar.	Rut.	Tit.	Leuc.	Zr.	Mz.	T. Ec.%	G. S.	H. Br.%
S1	0.43	0.83	0.22	0.10	0.08	0.13	0.130	0.090	0.007	2.017	2.970	4.987
S2	0.58	0.86	0.15	0.14	0.11	0.14	0.150	0.120	0.015	2.265	2.966	5.231
S3	0.48	0.63	0.11	0.15	0.03	0.10	0.120	0.073	0.023	1.716	2.797	4.513
S4	0.64	0.87	0.13	0.11	0.02	0.07	0.150	0.066	0.021	2.077	3.375	5.452
S5	0.55	0.79	0.16	0.21	0.16	0.08	0.130	0.150	0.042	2.275	3.288	5.563
S6	0.63	0.84	0.11	0.20	0.27	0.05	0.180	0.260	0.047	2.578	2.884	5.462
S7	0.66	0.82	0.23	0.38	0.28	0.09	0.200	0.340	0.043	3.039	1.456	4.495
S8	0.69	0.89	0.29	0.47	0.23	0.11	0.270	0.370	0.055	3.376	2.261	5.637
S9	0.76	0.92	0.34	0.54	0.27	0.19	0.310	0.400	0.057	3.787	1.947	5.734
S10	0.78	0.96	0.46	0.59	0.32	0.21	0.390	0.450	0.062	4.222	2.120	6.342
S11	0.87	1.08	0.48	0.68	0.36	0.15	0.410	0.530	0.074	4.634	1.887	6.521
S12	0.80	0.93	0.25	0.56	0.31	0.11	0.330	0.450	0.051	3.791	0.985	4.776
S13	0.65	0.81	0.19	0.35	0.21	0.07	0.230	0.310	0.040	2.860	1.362	4.222
S14	0.69	0.86	0.13	0.23	0.19	0.05	0.210	0.250	0.010	2.620	1.436	4.056
S15	0.58	0.81	0.09	0.20	0.11	0.05	0.140	0.230	0.008	2.218	2.005	4.223
Min.	0.430	0.630	0.090	0.100	0.020	0.045	0.120	0.066	0.007	1.716	2.340	4.056
Max.	0.870	1.080	0.480	0.680	0.360	0.210	0.410	0.530	0.074	4.634	1.887	6.521
Aveg.	0.653	0.860	0.223	0.327	0.197	0.106	0.223	0.273	0.037	2.898	2.249	5.148
W1	0.33	0.49	0.09	0.12	0.09	0.035	0.13	0.11	0.041	1.436	2.209	3.645
W2	0.31	0.47	0.11	0.15	0.11	0.073	0.14	0.15	0.052	1.565	2.294	3.859
W3	0.39	0.52	0.13	0.13	0.09	0.066	0.13	0.21	0.017	1.683	2.753	4.436
W4	0.34	0.51	0.12	0.12	0.13	0.053	0.11	0.18	0.016	1.579	3.052	4.631
W5	0.48	0.56	0.1	0.11	0.12	0.062	0.14	0.23	0.011	1.813	2.834	4.647
W6	0.32	0.54	0.09	0.13	0.16	0.043	0.11	0.24	0.063	1.696	2.648	4.344
W7	0.36	0.47	0.11	0.12	0.17	0.024	0.12	0.26	0.032	1.666	3.086	4.752
W8	0.29	0.43	0.16	0.14	0.14	0.055	0.14	0.25	0.065	1.670	2.568	4.238
W9	0.21	0.35	0.11	0.1	0.11	0.047	0.1	0.19	0.037	1.254	1.989	3.243
W10	0.3	0.48	0.12	0.09	0.1	0.031	0.11	0.21	0.022	1.463	2.614	4.077
Min.	0.2100	0.3500	0.0900	0.0900	0.0900	0.0240	0.1000	0.1100	0.0110	1.2540	1.9890	3.2430
Max.	0.4800	0.5600	0.1600	0.1500	0.1700	0.0730	0.1400	0.2600	0.0650	1.8130	2.9390	4.7520
Aveg.	0.3330	0.4820	0.1140	0.1210	0.1220	0.0489	0.1230	0.2030	0.0356	1.5825	2.6047	4.1872

Mag.=magnetite, Ilm.=ilmenite, Hem.=hematite, Gar.=garnet, Rut.=rutile, Tit.=titanite, Leuc.=Leucoxene, Zr.=zircon, Mz.=monazite, T. Ec.= total Economic minerals, G.S.= green silicates and H.Br.=heavy bromoform

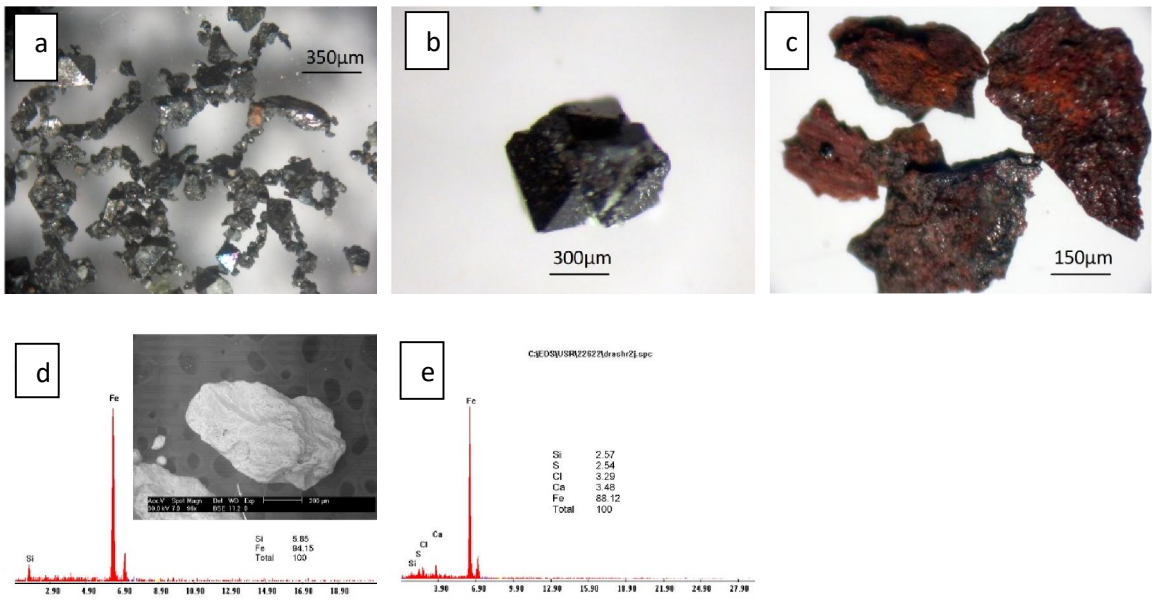


Fig. 6: Photomicrographs of magnetite grains show: a) Aggregates of angular, sub-angular and sub-rounded grains, b) octahedron crystals with parallel twining, c) different degrees of alteration, d& e) EDX and BSE image of magnetite grain

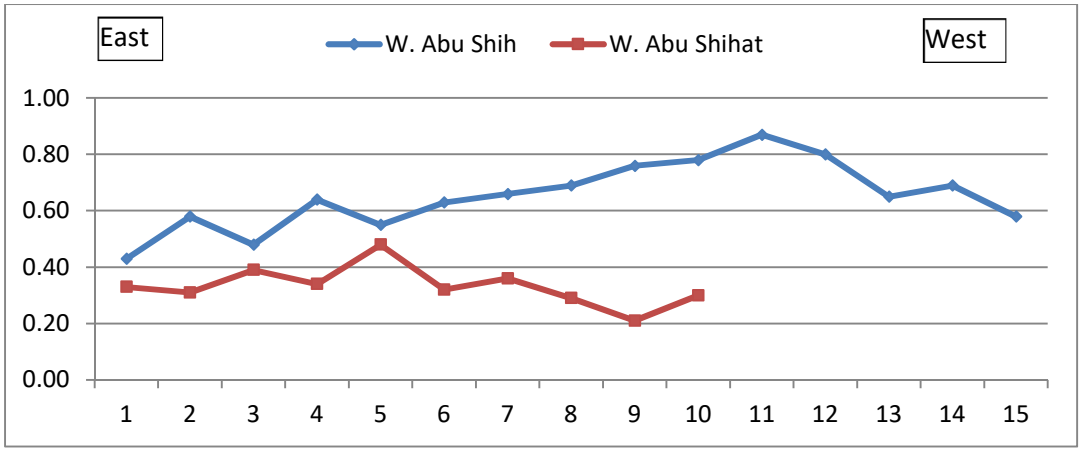


Fig. 7: Lateral distribution of magnetite.

Ilmenite $FeTiO_3$

Ilmenite is the most abundant Fe-Ti oxide mineral. Ilmenite represents the most frequent mineral relative to the heavy economic minerals in the studied sediments. It is rounded to sub-angular black grains with its characteristic purple sub-metallic luster. It occurs in a wide variety of igneous rocks, some metamorphic rocks, and as detritus mineral grains. Ilmenite was recorded as iron-black with metallic luster. It occurs as aggregates with different shapes (Fig.8a), triangular shape (Fig.8b) and some grains show reelects of groves as a result of the liberation from other minerals (Fig.8c). Picked pure ilmenite grains were investigated under the Environmental Scanning Electronic Microscope (ESEM) and the elemental chemical compositions are shows triangular shape (Fig.8d), Irregular shapes (Fig.8e), rounded to sub-rounded (Fig.8f) and groves (Fig.8g).

Ilmenite was recorded in all studied sediments and its content range from 0.63% to 1.08% with an average of 0.86% in wadi Abu Shih and range from 0.350% to 0.56% with an average of 0.482% in wadi Abu Shihat (Table 2).The lateral distribution of ilmenite percentages illustrated in (Fig. 9), and show the high concentration at the west and the middle parts beside G. Abu Shihat While the low concentration located at the eastern part in wadi Abu Shih while the concentration decrease gradually from the east to the west in wadi Abu Shihat.

Leucoxene ($FeTiO_3$)

Indeed, leucoxene is an alteration product of ilmenite and is the transition stage between ilmenite and the secondary rutile. It is composed mainly from minute crystals of brookite and anatase. The leucoxene commonly occurs as rounded grains, opaque in transmitted light. A rough pitted surface is the characteristic phenomena of most grains. The color of leucoxene varies from white, yellowish white to brown, it depends mainly on the degree of alteration. Ibrahim (1995) stated that, if the iron content decreases, the grain color becomes lighter brownish yellow, yellow, yellowish white and light creamy colors. Its grains range from irregular forms and colors, oval, rounded to sub-rounded and discoidal shapes with smooth or pitted surface (Fig. 10a). Ilmenite occurs as relicts on the surface of leucoxene indicating the alteration processes (Fig. 10b). Picked leucoxene grains were investigated using ESEM and their chemical composition shows rounded grains (Fig. 10c) and oval grains (Fig. 10d).

Leucoxene was recorded in all studied sediments and its content range from 0.12% to 0.41% with an average of 0.223% in wadi Abu Shih and range from 0.1% to 0.14% with an average of 0.123% in wadi Abu Shihat (Table 2).The lateral distribution of leucoxene percentages illustrated in (Fig. 11), and show the high concentration at the west and the middle parts beside G. Abu Shihat While the low concentration located at the eastern part in wadi Abu Shih while the concentration decrease gradually from the east to the west in wadi Abu Shihat

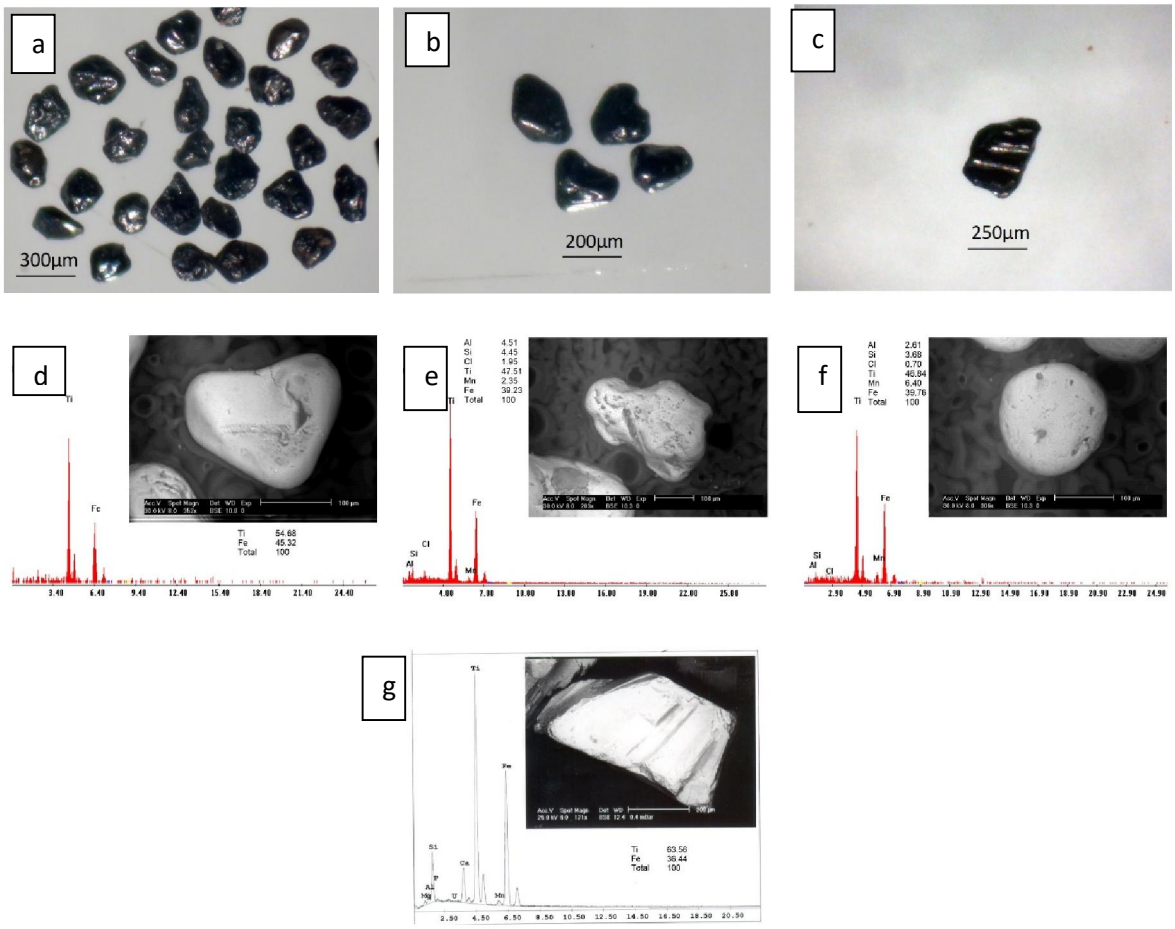


Fig. 8: Photomicrograph of ilmenite grains shows: a) aggregates with different shapes, b) triangular shape, c) groves. EDX and BSE image of ilmenite grains shows: d) Triangular shape, e) Irregular shapes, f) Rounded to sub-rounded and g) groves.

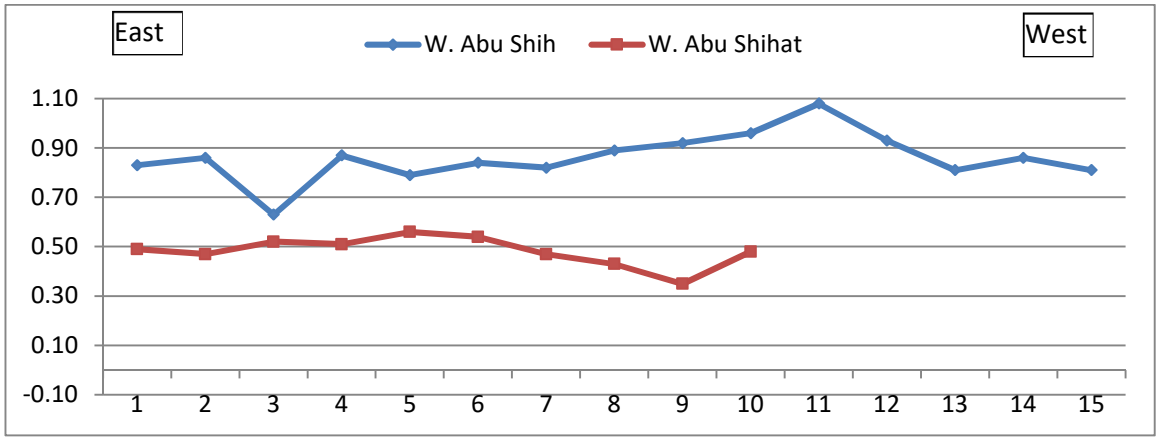


Fig. 9: Lateral distribution of ilmenite.

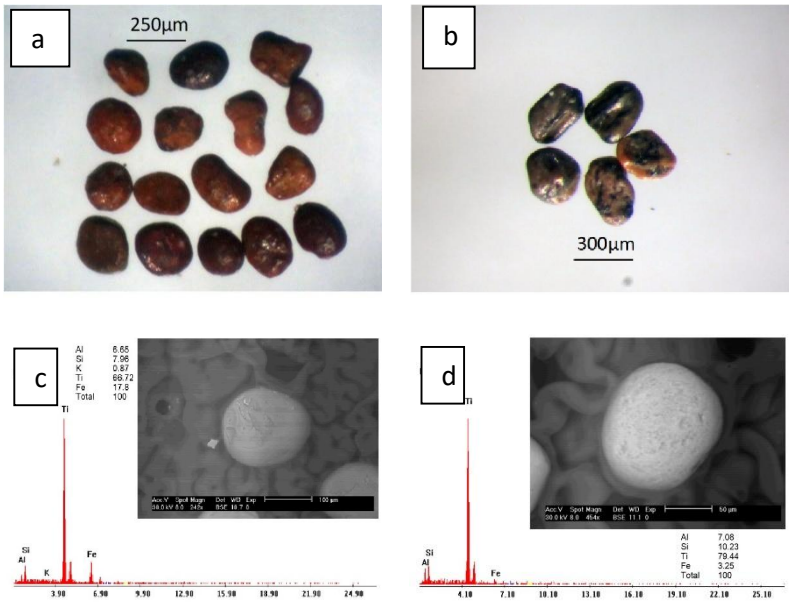


Fig. 10: Photomicrographs of leucoxene grains shows: a) Different forms and colors of leucoxene grains, and b) Residual ilmenite particles within leucoxene grains. EDX and BSE image of leucoxene grain shows: c) rounded grains and d) oval grains.

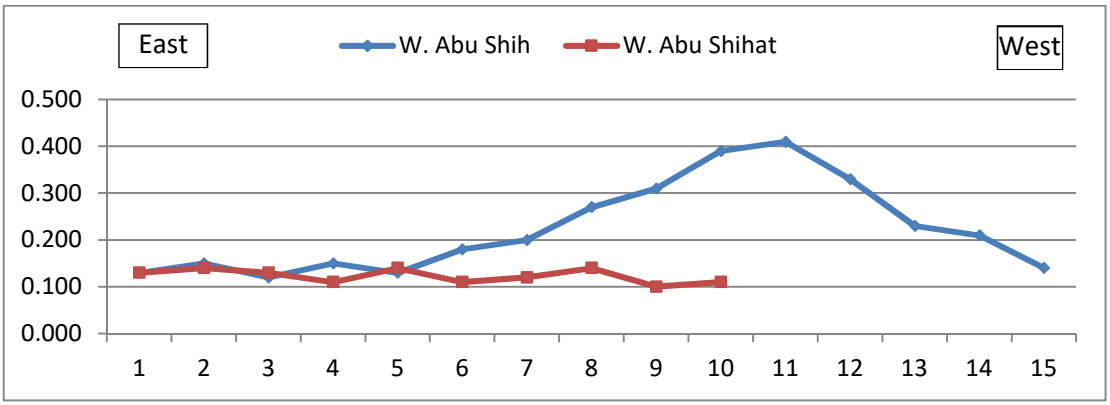


Fig. 11: Lateral distribution of leucoxene.

Hematite

Hematite is the principle ore of iron. Some hematite verities used in jewelry. It considers the alteration product of many Fe-bearing minerals especially pyrite and so-called hematite after pyrite or pseudomorphic pyrite (Fig. 12a). The non-crystalline forms of hematite are supposedly transformations of the mineral limonite. Hematite occurs as a reddish brown to black color (Fig. 12b&c), with metallic or dull in earthy. The different habits of pseudomorphic pyrite as recorded by ESEM were shown in (Fig. 12d).

Hematite was recorded in the most studied sediments and its content range from 0.09% to 0.48% with an average of 0.223% in wadi Abu Shih and range from 0.09% to 0.16% with an average of 0.114% in wadi Abu Shihat (Table 2).The lateral distribution of hematite percentages illustrated in (Fig. 13), and show the high concentration at the west and the middle parts beside G. Abu Shihat While the low concentration located at the eastern part in wadi Abu Shih while the concentration decrease gradually from the east to the west in wadi Abu Shihat.

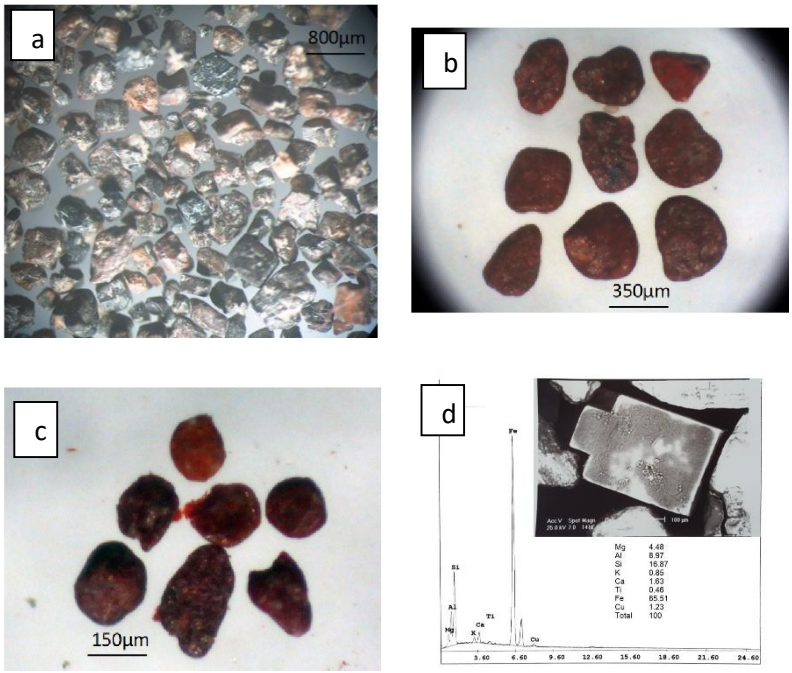


Fig. 12: Photomicrographs of hematite grains shows: a) hematite after pyrite, back) Different forms and colors of hematite grains and d) EDX and BSE image of hematite after pyrite.

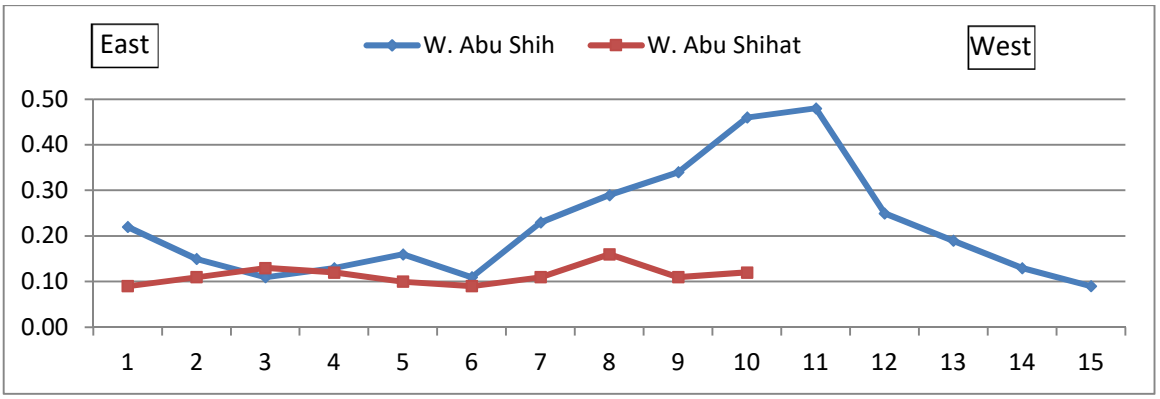


Fig. 13: Lateral distribution of hematite.

Non-opaque minerals

Zircon ($ZrSiO_4$)

Most of zircon grains have euhedral external morphology. Zircon separated in the nonmagnetic field 1.5A have long prismatic water clear color with vitreous luster. Armstrong (1922), Groves (1930), Poldervaart (1955-1956) and Saxena (1966) stated that the water clear zircon grains in all types of rocks are nonmagnetic. It was recorded as colorless short to long prismatic with or without bipyramidal termination (Fig. 14a), white prismatic with smooth curved edges (Fig. 14b), light yellow (Fig. 14c), red short prismatic with bipyramidal termination (Fig. 14d) and red color short prismatic grain showing outgrowth (Fig. 14e).

Picked zircon grains were investigated using ESEM and their chemical compositions are shows colorless long prismatic grain (Fig. 14f), white grain (Fig. 14g) and red short prismatic grain showing outgrowth (Fig. 14h).

Zircon was recorded in all studied sediments and its content range from 0.066% to 0.53% with an average of 0.273% in wadi Abu Shih and range from 0.11% to 0.26% with an average of 0.203% in wadi Abu Shihat (Table 2).The lateral distribution of zircon percentages illustrated in (Fig. 15), and show the high concentration at the west and the middle parts beside G. Abu Shihat While the low

concentration located at the eastern part in wadi Abu Shih while the concentration increase gradually from the east to the west in wadi Abu Shihat.

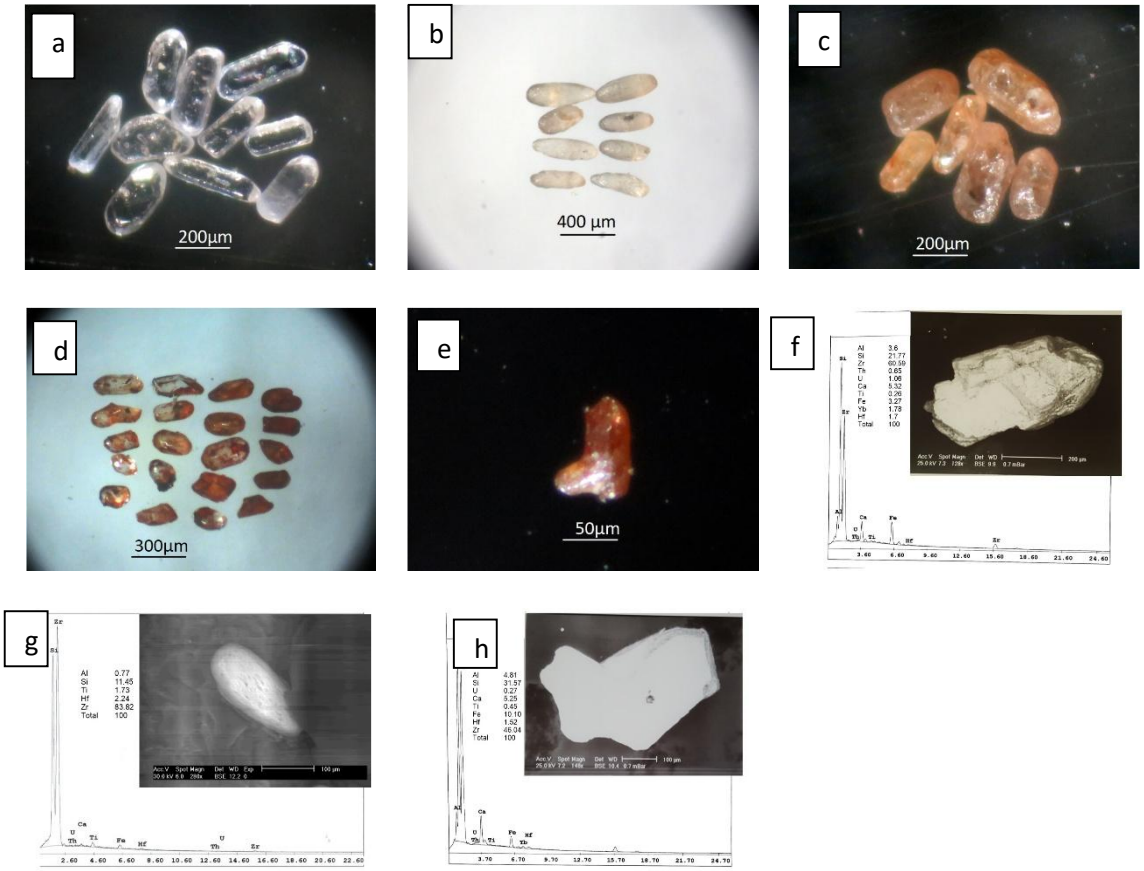


Fig. 14: Photomicrographs of zircon grains shows: a) Colorless short to long prismatic with or without bipyramidal termination, b) White prismatic with smooth curved edges, c) Light yellow oval grains, d) red short prismatic with bipyramidal termination and e) red color short prismatic grain showing outgrowth. EDX and BSE images of pure zircon grain shows: f) Colorless prismatic grain, g) white prismatic grain and h) red short prismatic grain showing outgrowth.

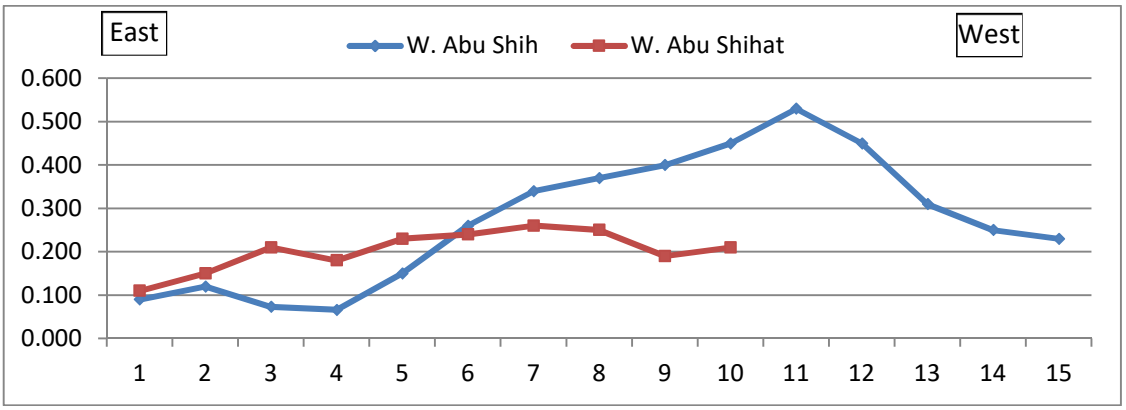


Fig. 15: Lateral distribution of zircon.

Garnet

The minerals of garnet group characterize some metamorphic rocks, others occur in high-pressure igneous rocks, and a major constituent of the Earth's mantle. Almandine type is the common garnet mineral in the studied samples. it was recorded in the studied samples as light rose, deep rose and red almandine grains (Fig. 16a&b). Picked garnet grains were investigated using ESEM and their chemical compositions are shows light rose almandine garnet (Fig. 16c) and deep rose almandine garnet (Fig. 16d) with ilmenite inclusion (Fig. 16e).

Garnet was recorded in all studied sediments and its content range from 0.1% to 0.68% with an average of 0.327% in wadi Abu Shih and range from 0.09% to 0.15% with an average of 0.121% in wadi Abu Shihat (Table 2).The lateral distribution of garnet percentages illustrated in (Fig. 17), and show the high concentration at the west and the middle parts beside G. Abu Shihat While the low concentration located at the eastern part in wadi Abu Shih while the concentration decrease gradually from the east to the west in wadi Abu Shihat.

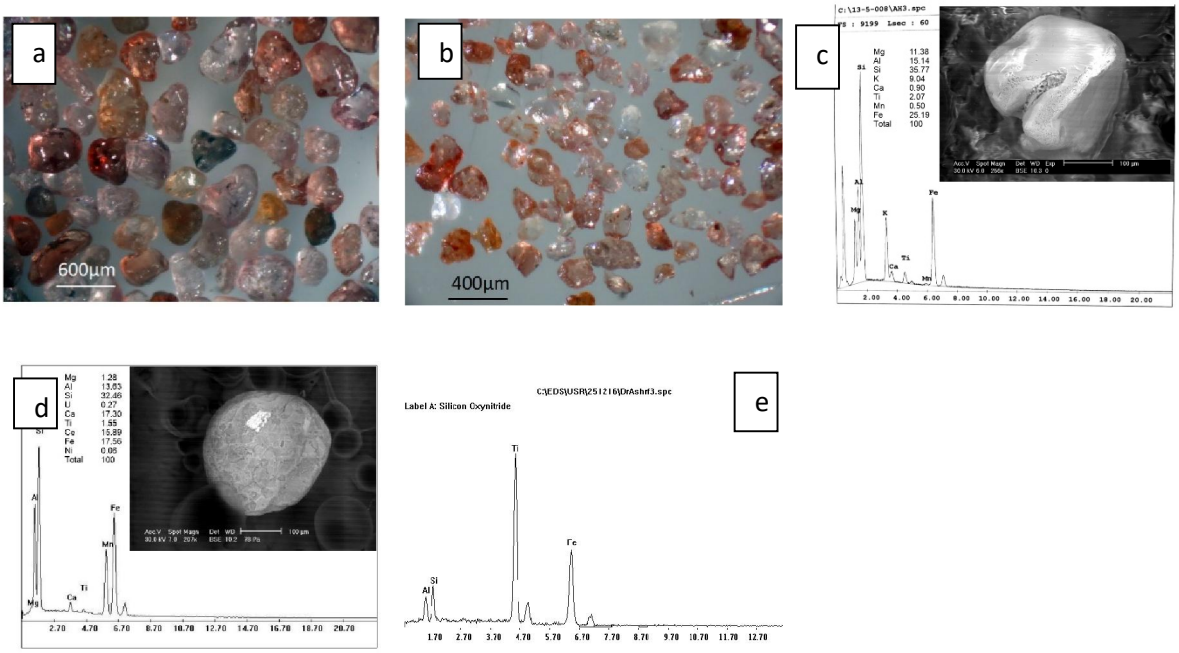


Fig. 16: Photomicrographs of garnet grains show: a& b) light rose, deep rose almandine grains and red almandine grains. EDX and BSE image of garnet shows : c) Light rose almandine garnet, d) Deep rose almandine garnet, e) ilmenite inclusion.

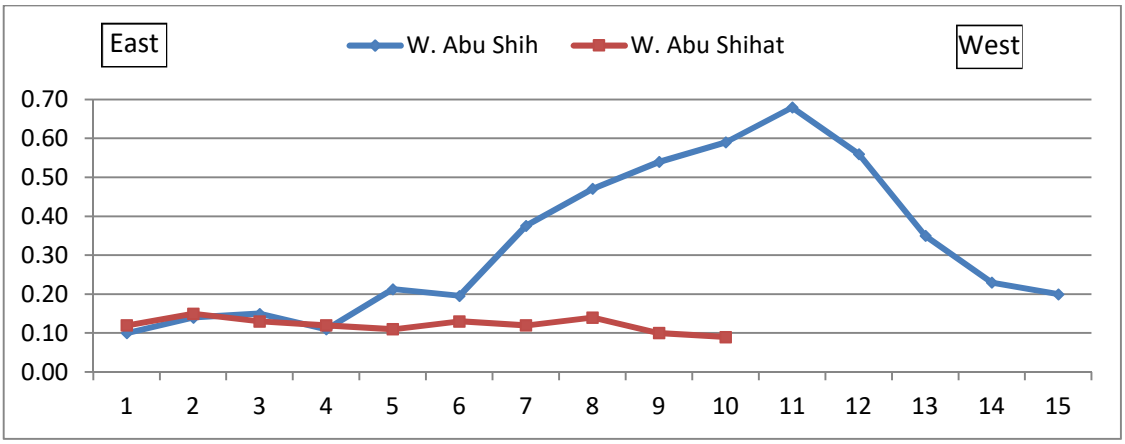


Fig. 17: Lateral distribution of garnet.

Monazite [$CeLaPO_4$]

Monazite is one of the most important nuclear minerals, being a major host for REEs and actinides Th and U (Hinton and Paterson, 1994; Bea *et al.,* 1994; Bea, 1996). The absorption spectrum of monazite is determined mainly by Nd and Pr elements, Fe3+, Fe2+ oxides content is the reason of coloration (Kravchenko, 1960). Most of these grains are characterized by pitted surfaces. Their color ranges from colorless, lemon yellow, light red to black (Fig. 18a). They occur as accessory mineral in the fine and very fine sand fractions. Monazite exhibits shape varies between rounded, discoidal and oval. Picked monazite grains were investigated using ESEM and their chemical compositions shows red oval grains (Fig. 18b).

Monazite was recorded in all studied sediments and its content range from 0.007% to 0.074% with an average of 0.037% in wadi Abu Shih and range from 0.011% to 0.065% with an average of 0.0356% in wadi Abu Shihat (Table 2).The lateral distribution of monazite percentages illustrated in (Fig. 19), and show the high concentration at the west and the middle parts beside G. Abu Shihat While the low concentration located at the eastern part in wadi Abu Shih while the concentration shows no trend in wadi Abu Shihat.

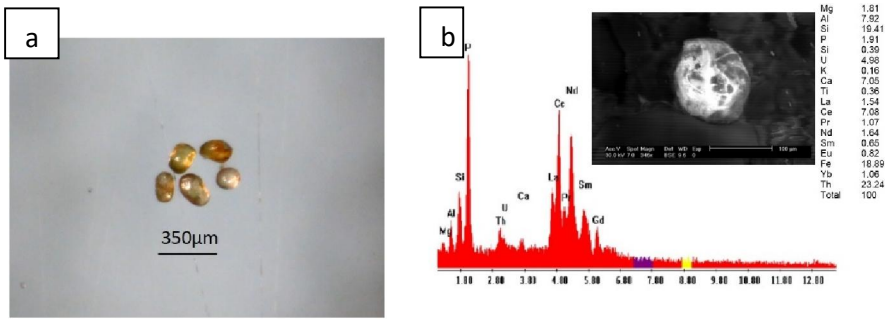


Fig. 18: a) Photomicrograph shows different shapes and colors of monazite grains and b) EDX and BSE image of monazite.

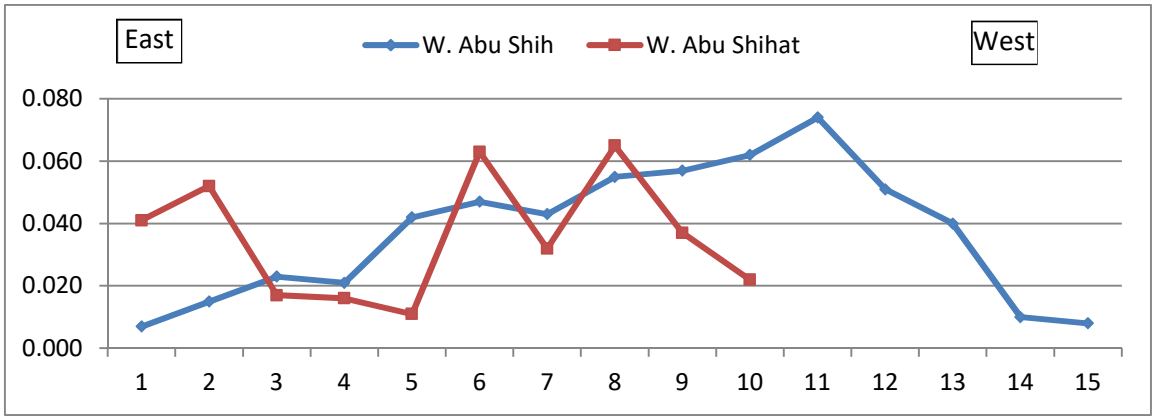


Fig. 19: Lateral distribution of monazite.

Rutile TiO_2

It is considered a major ore of titanium. Rutile occurs as red aggregates of different forms red to black prismatic grains (Fig. 20a), black massive granular, angular and sub-angular grains (Fig. 20b) and different colors of oval, semi-rounded to well-rounded and discoidal grains (Fig. 20c). Picked rutile grains were investigated using ESEM and their chemical compositions shows red to black prismatic grain (Fig. 20d).

Rutile was recorded in all studied sediments and its content range from 0.02% to 0.36% with an average of 0.197% in wadi Abu Shih and range from 0.09% to 0.17% with an average of 0.122% in wadi Abu Shihat (Table 2).The lateral distribution of rutile percentages illustrated in (Fig. 21), and show the high concentration at the west and the middle parts beside G. Abu Shihat While the low concentration located at the eastern part in wadi Abu Shih while the concentration increase gradually from the east to the west in wadi Abu Shihat.

Titanite (Sphene) Ca Ti Si O_5

Titanite is widespread in acidic in intermediate igneous rocks, and in several metamorphic rocks as accessory phase. It is more common in all samples of the studied sediments and its color varies from light Honey to dark honey grains (Fig.22a). Titanite mineral grains are subhedral to anhedral grains of adamantine luster. Picked titanite grains were investigated using ESEM and their chemical compositions are shown in figure (22b).

Titanite was recorded in all studied sediments and its content range from 0.045% to 0.21% with an average of 0.106% in wadi Abu Shih and range from 0.024% to 0.073% with an average of 0.0489% in wadi Abu Shihat (Table 2).The lateral distribution of titanite percentages illustrated in (Fig. 23), and show the high concentration at the west and the middle parts beside G. Abu Shihat While the low concentration located at the eastern part in wadi Abu Shih while the concentration decrease gradually from the east to the west in wadi Abu Shihat.

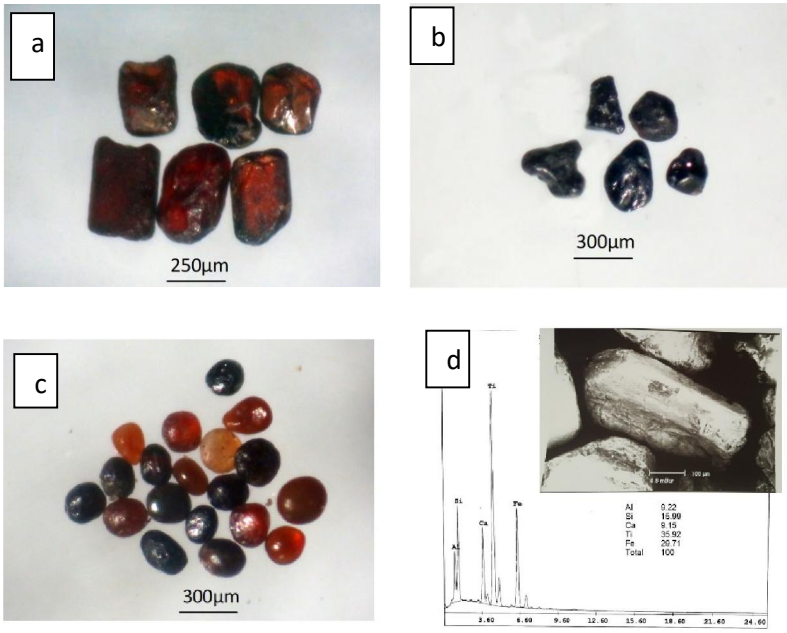


Fig. 20: Photomicrographs of rutile grains shows: a) Red prismatic grains, b) Black massive granular, angular and sub-angular grains, c) different colors of Oval, semi-rounded to well-rounded and discoidal grains, d) EDX and BSE image of rutile grains shows: a) red to black prismatic grain.

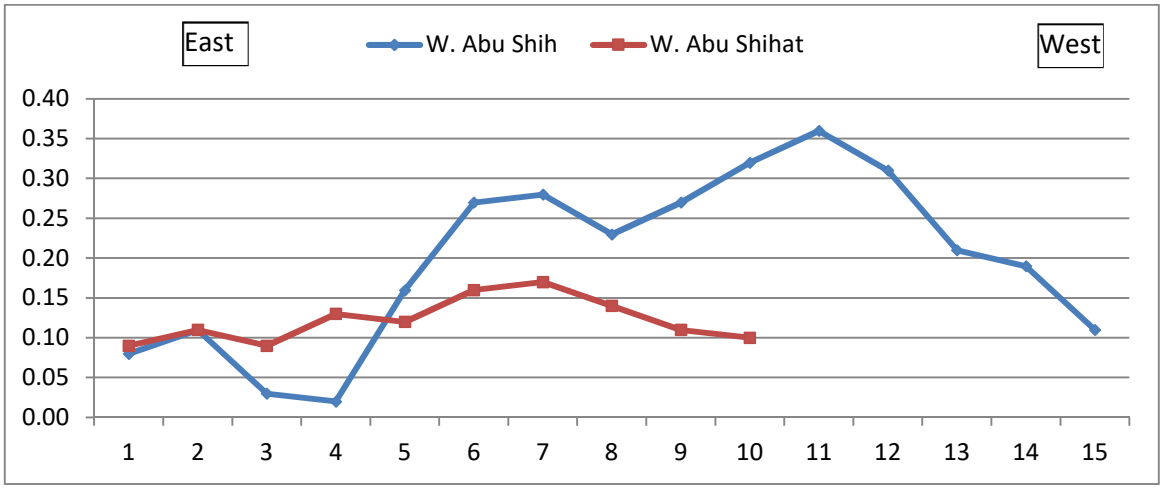


Fig. 21: Lateral distribution of rutile.

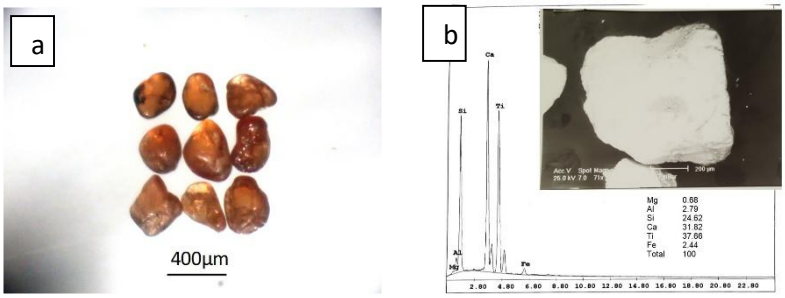


Fig. 22: a) Photomicrographs of light to dark Honey titanite grains and b) EDX and BSE image of titanite**.**

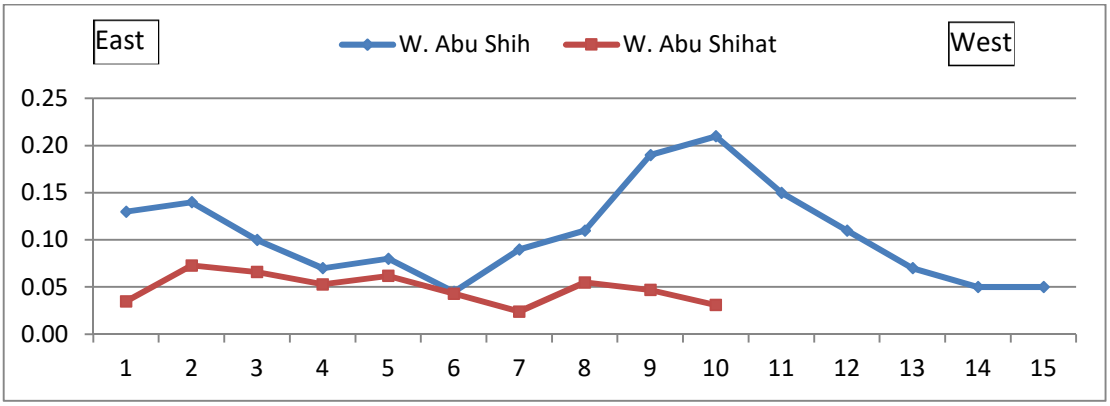


Fig. 23: Lateral distribution of titanite.

Radioactive Minerals

The radioactive minerals represented by Samarskit, Columbite, Fluorite and thorite. These minerals illustrated in the following paragraphs.

Samarskit (Oxides and Hydroxides) { (Y, Ce, U, Ca, Pb) (Nb, Ta, Sn)2O6}

It is present as accessory of many granitic pegmatites rich in rare earth elements and niobium. The crystals are rectangular black with brown surface alteration (Fig. 24a). Samarskit present in the middle part of Wadi Abu Shih samples. Picked Samarskit grains were investigated using ESEM and their chemical compositions are shown in figure (24b)

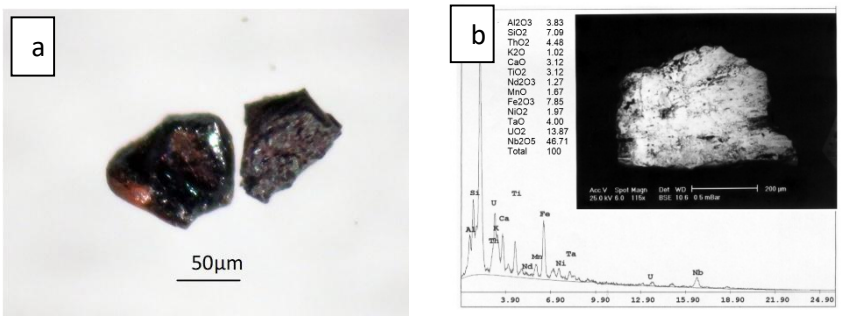


Fig. 24: a) Photomicrographs of black samarskite grains and b) EDX and BSE image of samarskite.

Columbite {(Fe, Mn) (Nb, Ta)2O6}

Columbite forms a series with the mineral tantalite as a semi-singular mineral called columbite-tantalite. They are the chief ores of niobium and tantalum. Columbite is the most widespread niobium which used in alloys for improved strength. Columbite is the more niobium rich end member and tantalite is the more tantalum rich end member. The two minerals of this series have similar properties since they have the same structure and similar chemistries. It displays several names according to the chemical composition which variable and depends on the Ta and Nb percentages in the solid solution such as ferrocolumbite, manganocolumbite, ferrotantalite and manganotantalite.

Columbite derived mainly from pegmatite, where it presents in wadi Abu Shih sediment samples of the middle and downstream area. It appears as prismatic, tabular or platy crystals, often in heart-shaped twins, striated, black with metallic appearance (Fig. 25a). Picked columbite grains were investigated using ESEM and their chemical compositions are shown in figure (25b).

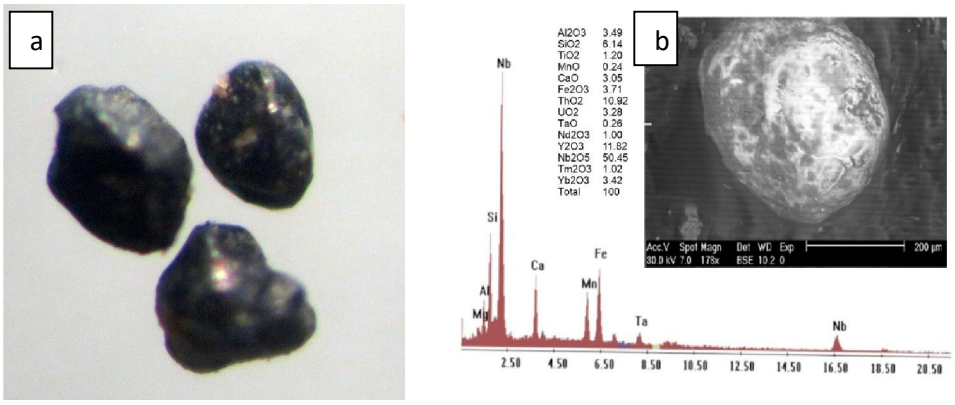


Fig. 25: a) Photomicrographs of black columbite grains and b) EDX and BSE image of columbite

Thorite

Thorite is the most common thorium silicate mineral presents as accessory mineral in different rock types and geological environments especially pegmatites, granites and hydrothermal deposits. It occurs associated with zircon, sphene, monazite, xenotime, allanite and various niobate-tantalates (Frondel, 1958). It is highly radioactive mineral due to the existence of thorium as a common radioactive element and uranium as minor component.

In the present study the separated grains of thorite occur as subhedral to anhedral form ranging in color from brownish black to black with greasy luster (Fig. 26a). Picked thorite grains were investigated using ESEM and their chemical compositions are shown in figure (26b).

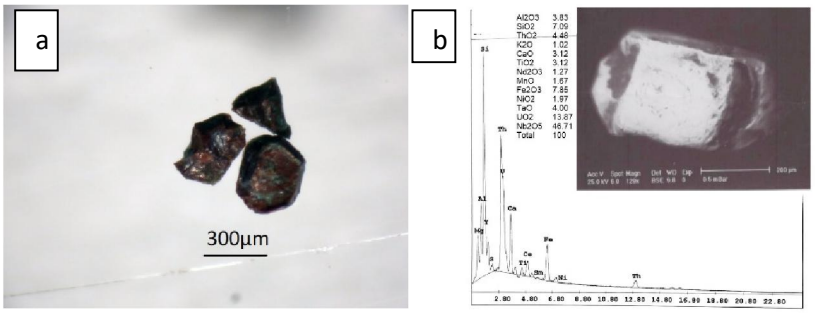


Fig. 26: a) Photomicrographs of brownish black thorite grains and b) EDX and BSE image of thorite

Fluorite

Fluorite occurs in different geological environments particularly in granites and pegmatites, and it has close geochemical association with U, Th and REE. Phiilips and Griffen (1981); Khazback and Raslan (1995); Sherif (1998); Hassaan (2005); Bishr (2007) remarked a positive relation between color of fluorite and the accompanying uranium minerals or to the presence of Y in particular (Fayziev, 1990). The granites enriched in uranium minerals usually contain fluorite crystals of blue, violet and deep violet or even black. The separated grains occur as massive and some grains are euhedral light violet with vitreous luster (Fig. 27a) and contain red inclusions. Picked thorite grains were investigated using

ESEM and their chemical compositions are shown in figure (27b), with thorite inclusions (Fig. 27c).

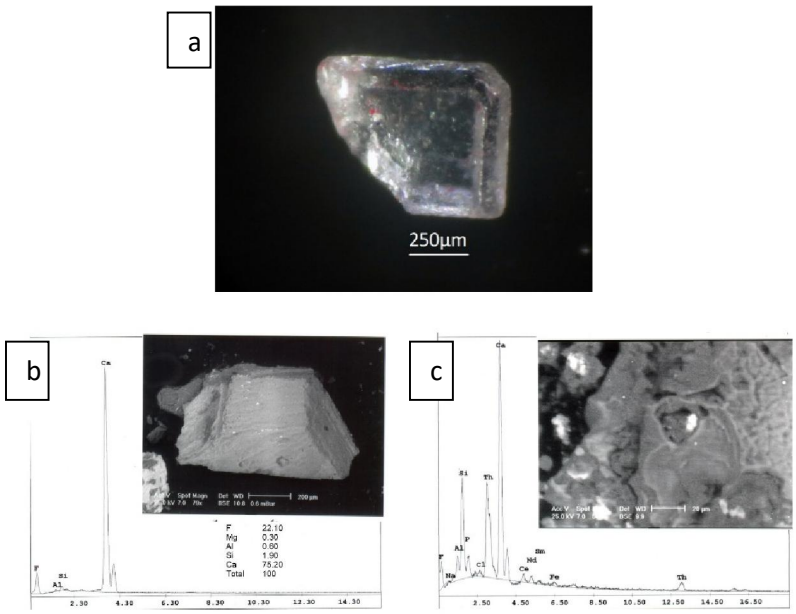


Fig. 27: a) Photomicrographs of light violate fluorite grains with red inclusions, b) EDX and BSE image of fluorite grain and c) thorite inclusions.

Accessory minerals

Pyrite

Pyrite used as a source of Sulphur for the manufacture of sulphuric acid. It is frequently rich in gold values and there for may be an important ore of gold. pyrite occurs as large subhedral to anhedral with yellow color (Fig. 28a) and euhedral grains (Fig. 28b) with metallic luster. Picked pyrite grains were investigated using ESEM and their chemical compositions are shown in figure (28c).

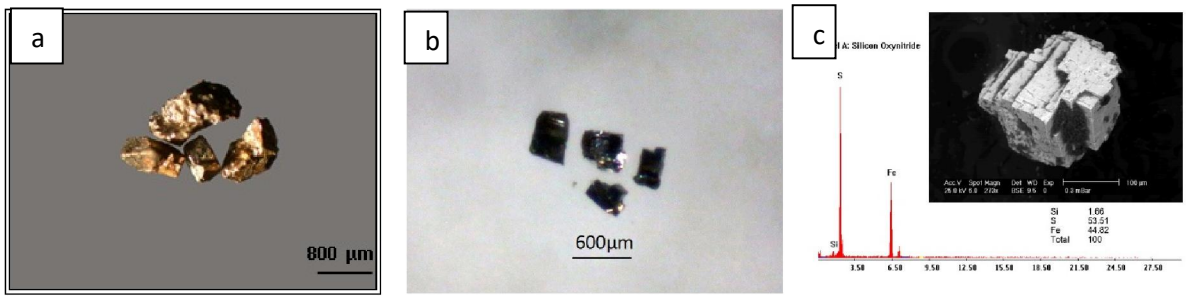


Fig. (28): Photomicrographs of pyrite grains shows: a) subhedral to anhedral with yellow color b) euhedral grains and c) EDX and BSE image of pyrite grain.

Apatite

Chlorapatite is the most common phosphate mineral occurs widely as an accessory mineral in igneous rocks and in calcium rich metamorphic rocks. It was recorded in the studied samples as wedge dark yellow grains (Fig. 29a). Picked apatite grains were investigated using ESEM and their chemical compositions are shown in figure (29b), which shows zircon inclusion (Fig. 29c.

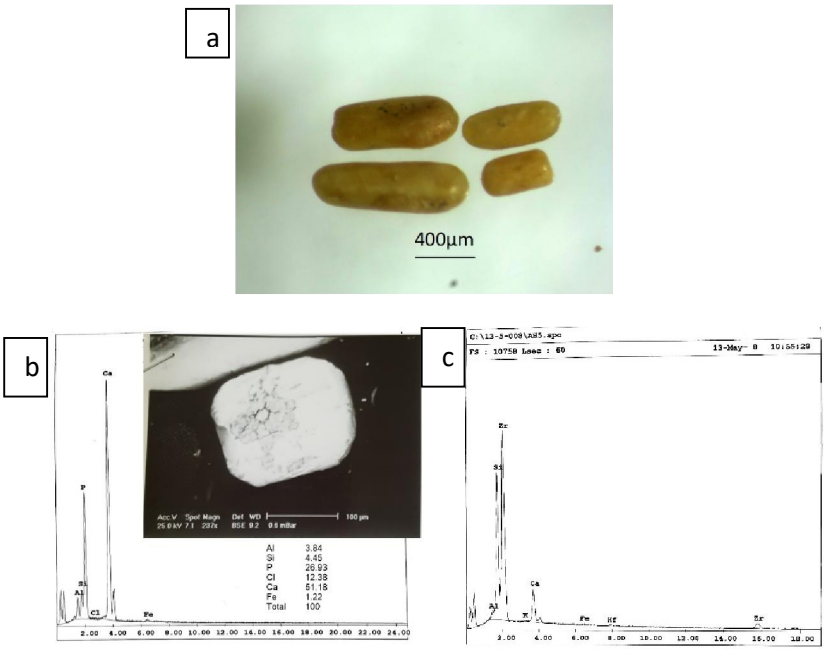


Fig. 29: a) Photomicrographs of dark yellow apatite grains, b) EDX and BSE image of apatite grain and c) zircon inclusion.

Atacamite

Atacamite was recorded in some samples of the studied area by rare trace non-magnetic minerals. It is a comparatively rare mineral, formed from primary copper minerals in the oxidation conditions. It has green color (Fig. 30a) with dull luster (Phillips and Griffen 1981. Picked apatite grains were investigated using ESEM and their chemical compositions are shown in figure (30b).

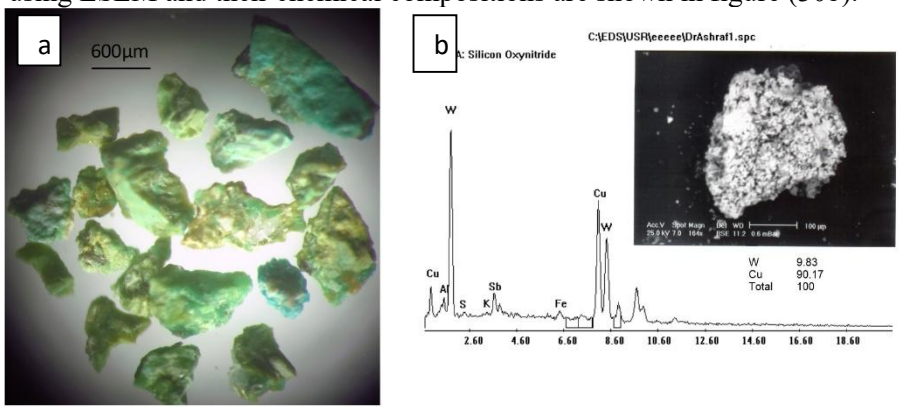


Fig. 30: a) Photomicrographs of green atacamite grains and b) EDX and BSE image of atacamite.

Cassiterite

Cassiterite (SnO_2) has been the chief tin ore throughout ancient history and remains the most important source of tin today due to their high durability. The majorities of cassiterite grains have black (Fig. 31a). Picked cassiterite grains were investigated using ESEM and their chemical compositions are shown in figure (31b).

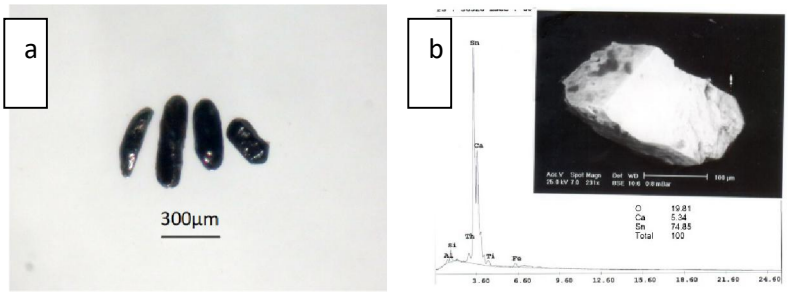


Fig. (31): a) Photomicrographs of black cassiterite grains and b) EDX and BSE image of cassiterite.

Radioactivity

A total of 25 stream sediment samples had been collected from the studied area throughout systematic sampling to determine their eU, eTh, eRa and K% contents. Wadi Abu Shih covered by 15 samples and wadi Abu Shihat covered by 10 samples (Fig. 4).

Determinations of the eU, eTh, Ra (ppm) and K (%) concentrations of the studied stream sediments were carried out using a Bicron Scintillation Detector NaI (TI) 76x76mm. They were packed in plastic containers, sealed carefully, and stored for thirty days prior to counting. The obtained results from the radiometric measurements of the studied stream sediments are listed in table 3.

The eU examined in the stream sediments of Wadi Abu Shih ranges from 4 ppm to 25 ppm, with an average 13.93 ppm, while eTh ranging from 12 ppm to 60 ppm, with an average 30.13 ppm, Ra ranging from 4 ppm to 19 ppm, with an average 8.53 ppm and K% ranging from 1.4% to 2.6 %, with an average 2.12%. The eU examined in the stream sediments of Wadi Abu Shihat ranges from 5 ppm to 9 ppm, with an average 6.5 ppm, while eTh ranging from 11 ppm to 16 ppm, with an average 13.7 ppm, Ra ranging from 5 ppm to 9 ppm, with an average 6.9 ppm and K% ranging from 1.1% to 3.3 %, with an average 1.91%. From these data can show the histograms for these elements as in figures (32) for wadi Abu Shih and figure (33) for wadi Abu Shihat.

Table 3: The distribution of radiometric measurements of the studied stream sediments samples

Sample No.	eU (ppm)	eTh (ppm)	Ra (ppm)	K (%)	Sample No.	eU (ppm)	eTh (ppm)	Ra (ppm)	K (%)
S1	7	19	5	2.4	**W1**	6	13	5	2.6
S2	5	18	7	2.6	**W2**	8	15	7	1.7
S3	8	14	4	1.4	**W3**	7	12	8	2.7
S4	4	23	6	1.4	**W4**	6	14	5	1.5
S5	7	12	4	1.8	**W5**	9	11	6	1.1
S6	5	21	9	2.3	**W6**	7	15	5	3.3
S7	14	23	7	2.1	**W7**	6	14	9	1.4
S8	19	34	8	2.6	**W8**	5	16	8	1.6
S9	22	49	19	2.3	**W9**	6	13	9	1.5
S10	25	39	7	2.2	**W10**	5	14	7	1.7
S11	24	60	14	2.1					
S12	21	47	8	1.5					
S13	21	30	10	2.4					
S14	16	34	14	2.5					
S15	11	29	6	2.2					
Min.	4	12	4	1.4	**Min.**	5	11	5	1.1
Max.	25	60	19	2.6	**Max.**	9	16	9	3.3
Aveg.	13.93	30.13	8.53	2.12	**Aveg.**	6.50	13.70	6.90	1.91

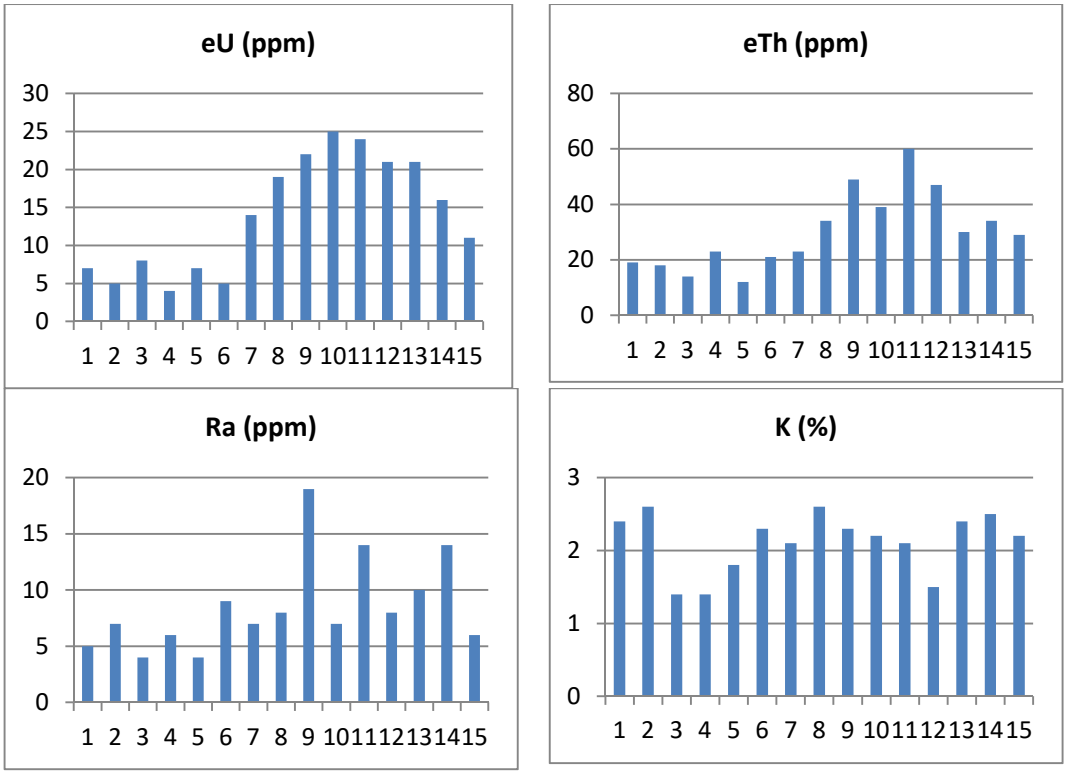


Fig. 32: Histograms of wadi Abu Shih showing the distribution of equivalent uranium ppm, equivalent thorium ppm, equivalent radium ppm and equivalent K%.

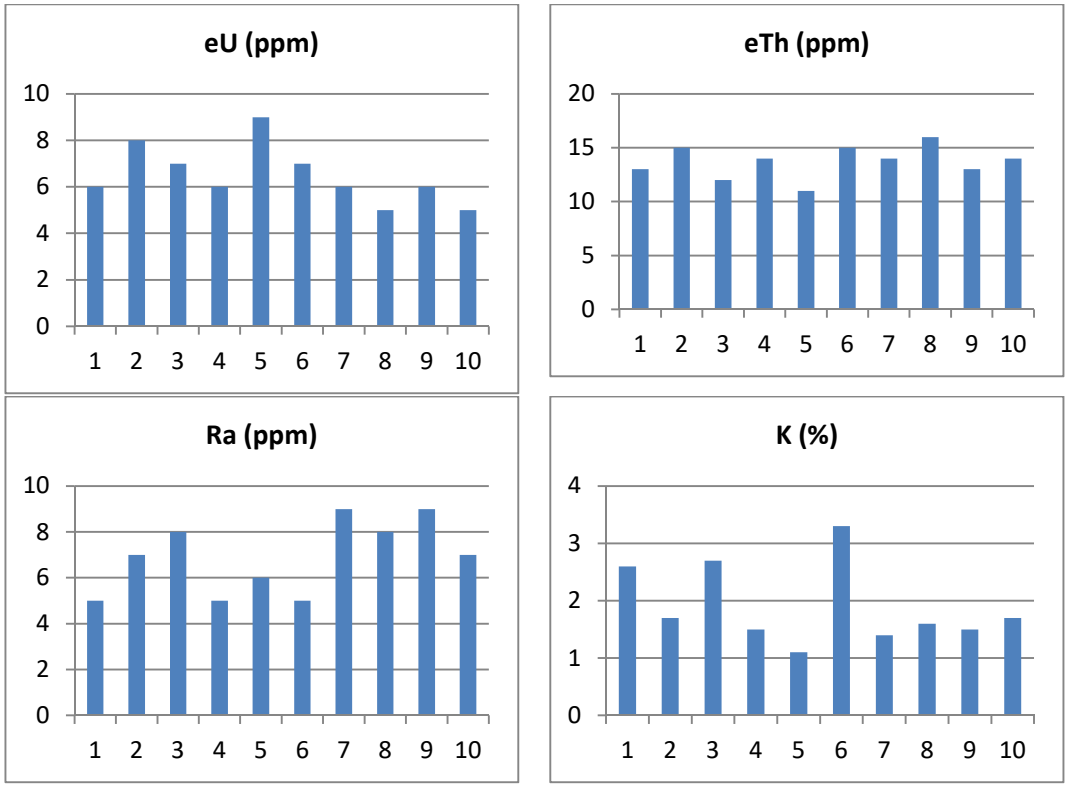


Fig. 33: Histograms of wadi Abu Shihat showing the distribution of equivalent uranium ppm, equivalent thorium ppm, equivalent radium ppm and equivalent K%

eU versus eTh variation diagram

The relation between eU and eTh may indicate the enrichment or depletion of U because Th is normally stable. Thorium is three times as abundant as uranium in all rock types. When this ratio is disturbed, it indicates either depletion or enrichment of uranium.

The eU against eTh variation diagram for the studied samples in wadi Abu Shih (Fig. 34a) indicates strong positive relationships between these two elements. This result explains the low leaching processes affecting on these samples. The eU against eTh variation diagram for the studied samples in wadi Abu Shihat (Fig. 34b) indicates strong negative relationships between these two elements. This result explains the high leaching processes affecting on these samples.

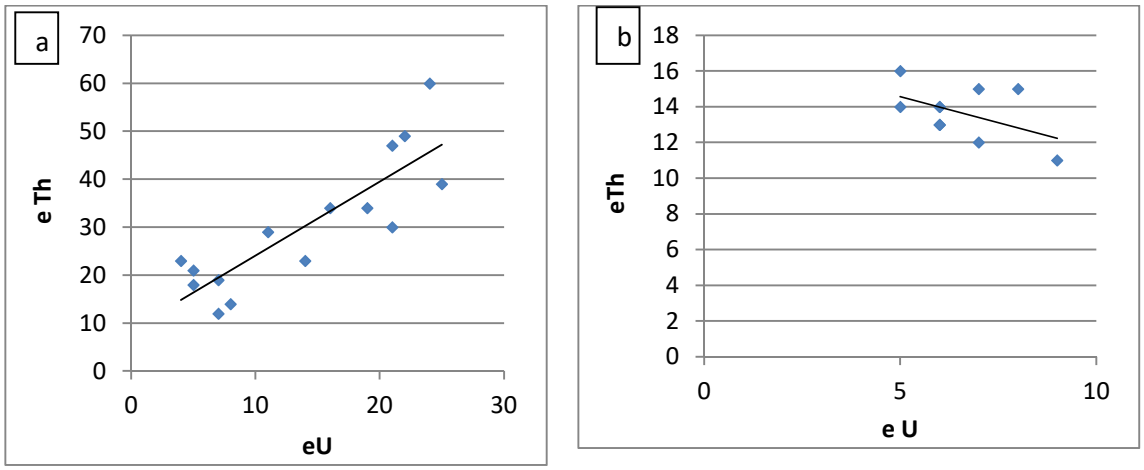


Fig. 34: Variation diagram shows: a) the relation between eU and eTh in wadi Abu Shih and b) the relation between eU and eTh in wadi Abu Shihat.

eU, and eTh versus eRa variation diagram

These relations illustrated by figures 35 and show direct relation between them and explains the low alteration processes affecting on these samples.

The eU against eRa variation diagram for the studied samples in wadi Abu Shih (Fig. 35a) indicates strong positive relationships between these two elements. This result explains the low leaching processes affecting on these samples. The eU against eRa variation diagram for the studied samples in wadi Abu Shihat (Fig. 35b) indicates strong negative relationships between these two elements. This result explains the high leaching processes affecting on these samples.

The eTh against eRa variation diagram for the studied samples in wadi Abu Shih (Fig. 35c) indicates strong positive relationships between these two elements. This result explains the low leaching processes affecting on these samples. The eTh against eRa variation diagram for the studied samples in wadi Abu Shihat (Fig. 35d) indicates nearly horizontal relationships between these two elements.

eU versus Zr variation diagram

The eU versus Zr variation diagram in wadi Abu Shih (Fig. 36a) shows strong positive correlation in the studied samples. The uranium and zircon enrichment in the studied samples, supports the concept that U was trapped in the accessory minerals particularly zircon. The eU versus Zr variation diagram in wadi Abu Shihat (Fig. 36b) shows nearly horizontal correlation in the studied samples.

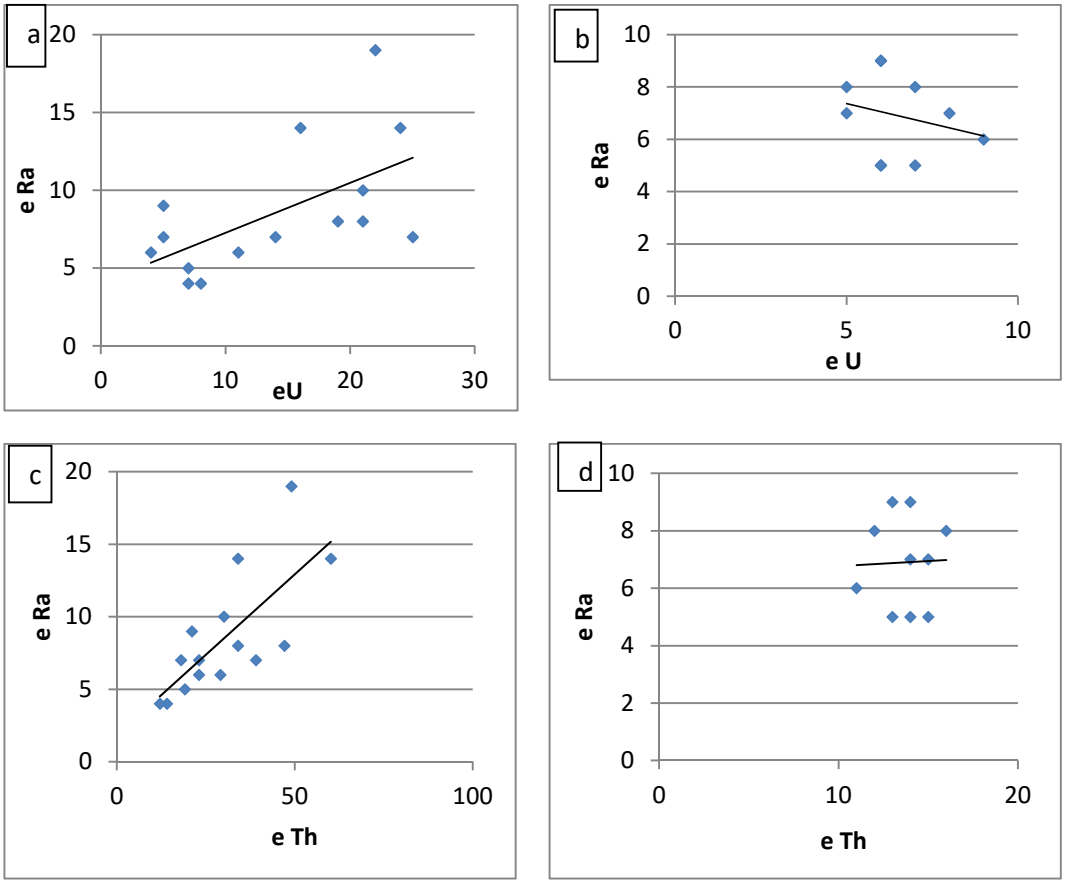


Fig. 35: variation diagram shows: a) the relation between eRa and eTh in wadi Abu Shih, b) the relation between eRa and eTh in wadi Abu Shihat, c) The relationship between e U and e Ra in wadi Abu Shih and d) The relationship between e U and e Ra in wadi Abu Shihat.

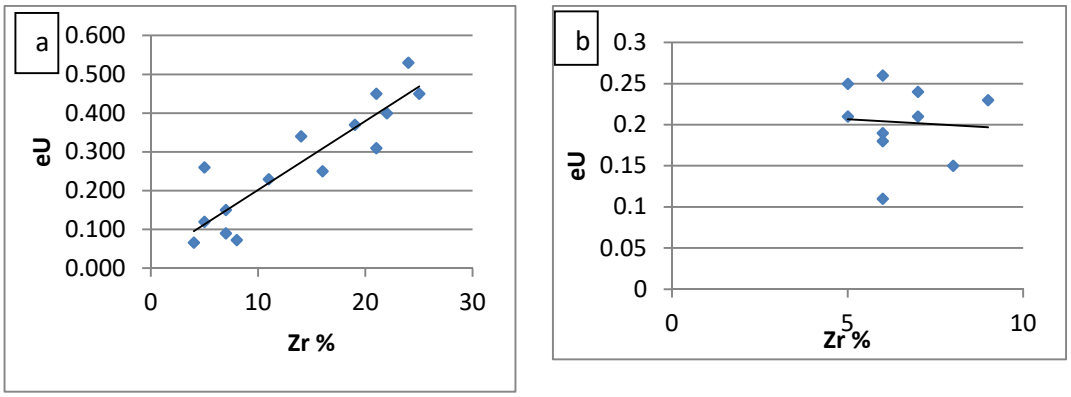


Fig. 36: variation diagrams shows: a) the relation between Zr% and eU in wadi Abu Shih, b) the relation between Zr% and eU in wadi Abu Shihat.

4. Conclusions

The area covered by basement rocks represented by metavolcanics, older granite, younger gabbro, and younger granite. The area covered by 25 samples of stream sediments, Wadi Abu Shih covered by 15 samples and wadi Abu Shihat covered by 10 samples. These sediments analyses by heavy liquid (bromoform 2.88 Sp.gr.). The total heavy minerals ranging from 4.056% to 6.521% with an average of about 5.148% in wadi Abu Shih and ranging from 3.243% to 4.752% with an average of about 4.187% in wadi Abu Shihat.

The total heavy economic minerals ranging from 1.716% to 4.634% with an average of about 2.898% in wadi Abu Shih and ranging from 1.254% to 1.813% with an average of about 1.5825% in wadi Abu Shihat. Magnetite range from 0.43% to 0.87% with an average of 0.653% in wadi Abu Shih

and range from 0.21% to 0.48% with an average of 0.333% in wadi Abu Shihat, ilmenite range from 0.63% to 1.08% with an average of 0.86% in wadi Abu Shih and range from 0.350% to 0.56% with an average of 0.482% in wadi Abu Shihat, leucoxene range from 0.12% to 0.41% with an average of 0.223% in wadi Abu Shih and range from 0.1% to 0.14% with an average of 0.123% in wadi Abu Shihat, Hematite range from 0.09% to 0.48% with an average of 0.223% in wadi Abu Shih and range from 0.09% to 0.16% with an average of 0.114% in wadi Abu Shihat, Zircon range from 0.066% to 0.53% with an average of 0.273% in wadi Abu Shih and range from 0.11% to 0.26% with an average of 0.203% in wadi Abu Shihat, Garnet range from 0.1% to 0.68% with an average of 0.327% in wadi Abu Shih and range from 0.09% to 0.15% with an average of 0.121% in wadi Abu Shihat, Monazite range from 0.007% to 0.074% with an average of 0.037% in wadi Abu Shih and range from 0.011% to 0.065% with an average of 0.0356% in wadi Abu Shihat, Rutile range from 0.02% to 0.36% with an average of 0.197% in wadi Abu Shih and range from 0.09% to 0.17% with an average of 0.122% in wadi Abu Shihat and Titanite range from 0.045% to 0.21% with an average of 0.106% in wadi Abu Shih and range from 0.024% to 0.073% with an average of 0.0489% in wadi Abu Shihat.

Although the average of the total heavy minerals in wadi Abu Shih nearly close to that found in wadi Abu Shihat, we found the average of the economic minerals in wadi Abu Shih more than twice that found in wadi Abu Shihat. So, the economic heavy minerals restricted in wadi Abu Shih especially from sample S7 to sample S13.

The radioactive minerals represented by samarskite, thorite, columbite and fluorite. The eU examined in the stream sediments of Wadi Abu Shih ranges from 4 ppm to 25 ppm , with an average 13.93 ppm, while eTh ranging from 12 ppm to 60 ppm, with an average 30.13 ppm, Ra ranging from 4 ppm to 19 ppm, with an average 8.53 ppm and K% ranging from 1.4% to 2.6 %, with an average 2.12%. The eU examined in the stream sediments of Wadi Abu Shihat ranges from 5 ppm to 9 ppm , with an average 6.5 ppm, while eTh ranging from 11 ppm to 16 ppm, with an average 13.7 ppm, Ra ranging from 5 ppm to 9 ppm, with an average 6.9 ppm and K% ranging from 1.1% to 3.3 %, with an average 1.91%.

The variation diagrams between radioactive elements shows the low alteration processes affecting on the samples in wadi Abu Shih while shows the high alteration processes affecting on the samples in wadi Abu Shihat.

References

Abdel Ghani, I. M., 2001. Geology, petrology and radioactivity of Gabal El-Urf area, Central Eastern Desert, Egypt. Ph.D. Thesis, South Valley Univ., Qena, Egypt, 273 p.

Anas, M. E., 2015. Mineralogical and radioactive characterization of Gabal El-Urf pegmatites, Central Eastern Desert, Egypt. Al-Azhar Bull. Sci., 26(2):85-96.

Armstrong, P., 1922. Zircon as a criterion of igneous or metamorphic origin. Am. J. Sci., 4(23):391-395.

Asran, A. M. H., M. M. El-Mansi, M. E. Ibrahim and I. M. Abdel Ghani, 2013. Pegmatites of Gabal El-Urf, Central Eastern Desert, Egypt. The 7th Int. Conf. Geol. Afr., Assiut Univ., Egypt, IV:1-22.

Bea, F., 1996. Residence of REE, Y, Th and U in granites and crustal protoliths; implications for the chemistry of crustal melts. J. Petrol., 37(3):521-552.

Bea, F., M. D. Pereira, L. G. Corretgé and G. B. Fershtater, 1994. Differentiation of strongly peraluminous, perphosphorus granites: The Pedrobernardo pluton, Central Spain. Geochim. Cosmochim. Acta, 58(12):2609-2627.

Bishady, A. M., M. Y. Atawiya, G. H. Attia and A. A. El-Nahas, 1999. Petrographical and geochemical studies on Abu Zawal pegmatites and their host rocks, Central Eastern Desert, Egypt. The 4th Int. Conf. Geol. Arab World (GAW4), Cairo Univ., Egypt, 1:222-245.

Bishr, A. H. A., 2007. Factors controlling mineralizations of some shear zones in granites, South Sinai, Egypt. Ph.D. Thesis, Fac. Sci., Zagazig Univ., Egypt.

El Dabe, M. M., A. M. Ismail and M. Metwaly, 2022a. Geology and radioactivity of the pegmatite rocks of Gabal El-Urf, Northern Eastern Desert, Egypt. J. Rad. Nucl. Appl., 7(1):1-13.

El Dabe, M. M., A. M. Ismail, M. Metwaly, S. A. Taalab, M. Y. Hanfi and A. Ene, 2022b. Hazards of radioactive mineralization associated with pegmatites used as decorative and building material. Materials, 15(4):1224.

El-Gaby, S. and M. Habib, 1982. Geology of the area southwest of Port Safaga, with special emphasis on the granitic rocks, Eastern Desert, Egypt. Ann. Geol. Surv. Egypt, 12:47-71.

El-Mansi, M. M. and A. M. Dardier, 2005. Contribution to the geology and radioactivity of the older granitoids and younger granites of Gabal El-Urf–Gabal Abu Shihat area, Eastern Desert, Egypt. Delta J. Sci., 29:1-17.

El-Taher, M. A., 1978. Relation between geology and radioactivity of some basement rocks to the north of Qena-Safaga Asphaltic Road, Eastern Desert, Egypt. M.Sc. Thesis, Fac. Sci., Al-Azhar Univ., Egypt, 101 p.

Fayziev, A. R., 1990. Yttrium in fluorite from endogenous mineral occurrences in the USSR. Geokhimiya, 7:1037-1042.

Flinter, B. H., 1959. The magnetic separation of some alluvial minerals in Malaya. Am. Mineral., 44(7-8):738-751.

Folk, R. L., 1980. Petrology of Sedimentary Rocks. Hemphill Publishing Company, Austin, Texas, USA, 184 p.

Frondel, C., 1958. Systematic mineralogy of uranium and thorium. U.S. Geol. Surv. Bull., 1064:1-400.

Groves, A. W., 1930. The heavy mineral suites and correlation of the granites of Northern Brittany, the Channel Islands, and the Cotentin. Geol. Mag., 67(5):218-240.

Habib, M. E., 1982. Landsat investigation of mineralized granites in the area between Gabal El Urf and El Eradiya west of Safaga, Egypt. Proc. 8th Int. Symp. Machine Process. Remotely Sensed Data, Purdue Univ., West Lafayette, Indiana, USA, 441-446.

Habib, M. E., 1987. Microplate accretion model for the Pan-African basement between Qena-Safaga and Qift-Quseir roads, Egypt. Bull. Fac. Sci., Assiut Univ., 16(1):199-239.

Hassaan, A. H. A., 2005. Evaluation of the heavy minerals in the coastal sand dunes, East Sabkhat El-Tina, North Sinai, Egypt. Ph.D. Thesis, Fac. Sci., Ain Shams Univ., Egypt.

Hinton, R. W. and B. A. Paterson, 1994. Crystallization history of granitic magma: Evidence from trace element zoning. Mineral. Mag., 58A(1):416-417.

Ibrahim, M. I. M., 1995. Investigation of some physical properties of zircon and rutile to prepare high purity mineral concentrates from the black sand deposits. M.Sc. Thesis, Mansoura Univ., Egypt.

Khamis, H. A., 2012. Structural and radiometric studies of the Precambrian rocks of Wadi Fatira El Zarqa area, Central Eastern Desert, Egypt. Ph.D. Thesis, Fac. Sci., Cairo Univ., Egypt, 299 p.

Khazback, A. E. and M. F. Raslan, 1995. Potentialities of physical up-grading of Gebel Gattar uranium ore, Eastern Desert, Egypt. Al-Azhar Bull. Sci., 5:1-7.

Kravchenko, G. T., 1960. Coloration of monazite. Izv. Sib. Otd. Akad. Nauk SSSR, 7:80-90.

Mohamed, S. S. M., 1998. Radioactivity and mineralogical studies on Wadi Abu Dabbab alluvial deposits, Central Eastern Desert, Egypt. M.Sc. Thesis, Fac. Sci., Ain Shams Univ., Egypt, 204 p.

Phillips, W. R. and D. T. Griffen, 1981. Optical Mineralogy: The Nonopaque Minerals. W. H. Freeman and Company, San Francisco, USA, 677 p.

Poldervaart, A., 1955. Zircon in rocks. 1. Sedimentary rocks. Am. J. Sci., 253(8):433-461.

Poldervaart, A., 1956. Zircon in rocks. 2. Igneous rocks. Am. J. Sci., 254(9):521-554.

Saxena, S. K., 1966. Evolution of zircon in sedimentary and metamorphic rocks. Sedimentology, 6(1):1-33.

Sherif, H. M. Y., 1998. Geology and uranium potentiality of Wadi Seih area, Southwest Sinai, Egypt. Ph.D. Thesis, Cairo Univ., Giza, Egypt, 229 p.